SANDIA REPORT

SAND2015-10871
Unlimited Release
Printed January, 2016

A Reduced Order Model of Force Displacement Curves for the Failure of Mechanical Bolts in Tension

Keegan J. Moore and Matthew R. W. Brake

Prepared by
Sandia National Laboratories
Albuquerque, New Mexico 87185 and Livermore, California 94550

Sandia National Laboratories is a multi-program laboratory managed and operated by Sandia Corporation, a wholly owned subsidiary of Lockheed Martin Corporation, for the U.S. Department of Energy's National Nuclear Security Administration under contract DE-AC04-94AL85000.

Sandia National Laboratories

Issued by Sandia National Laboratories, operated for the United States Department of Energy by Sandia Corporation.

Available to DOE and DOE contractors from
U.S. Department of Energy
Office of Scientific and Technical Information
P.O. Box 62
Oak Ridge, TN 37831

Telephone: (865) 576-8401
Facsimile: (865) 576-5728
E-Mail: reports@adonis.osti.gov
Online ordering: http://www.osti.gov/bridge

Available to the public from
U.S. Department of Commerce
National Technical Information Service
5285 Port Royal Rd
Springfield, VA 22161

Telephone: (800) 553-6847
Facsimile: (703) 605-6900
E-Mail: orders@ntis.fedworld.gov
Online ordering: http://www.ntis.gov/help/ordermethods.asp?loc=7-4-0#online

SAND2015-10871
Unlimited Release
Printed January, 2016

A Reduced Order Model of Force Displacement Curves for the Failure of Mechanical Bolts in Tension

Keegan J. Moore[1,2] and Matthew R. W. Brake,[1]

[1] Component Science and Mechanics
Sandia National Laboratories
MS 1070; P.O. Box 5800
Albuquerque, NM 87185-1070

[2] Department of Mechanical Science and Engineering
University of Illinois at Urbana-Champaign
1206 W. Green St.
Urbana, IL 61801, USA

Abstract

Assembled mechanical systems often contain a large number of bolted connections. These bolted connections (joints) are integral aspects of the load path for structural dynamics, and, consequently, are paramount for calculating a structure's stiffness and energy dissipation properties. However, analysts have not found the optimal method to model appropriately these bolted joints. The complexity of the screw geometry causes issues when generating a mesh of the model. This report will explore different approaches to model a screw-substrate connection. Model parameters such as mesh continuity, node alignment, wedge angles, and thread to body element size ratios are examined. The results of this study will give analysts a better understanding of the influences of these parameters and will aide in finding the optimal method to model bolted connections.

Acknowledgment

The authors would like to thank Gustavo Castelluccio, Jhana Gearhart, Tom Bosiljevac, Doug VanGoethem, Jeff Smith, and Jill Blecke for useful discussions regarding the failure of fasteners. Additionally, we would like to thank Mike Chiesa and Arthur Brown for their support through the ASC program.

Contents

Appendix

Figures

Tables

1 Introduction

The accurate prediction of the failure of fasteners due to external loads is a critical capability for the simulation of assembled structures. One pressing challenge, though, is the methodology for incorporating fasteners into a finite element simulation. In typical assemblies, there are dozens of, if not more, fasteners, each requiring tens of thousands of elements in a suitably refined mesh that includes contact and frictional interfaces. Further, there is no clear consensus on the manner in which to introduce preloads (i.e. via thermal loads, nonlinear static simulations, axial loads, etc.) (Kim, Yoon, and Kang 2007). The complexity that fasteners introduce into a high fidelity finite element model, therefore, is prohibitively expensive – another approach is necessitated.

This research focuses on the development of a single degree of freedom constitutive model to be used as a surrogate for high fidelity finite element modeling of fasteners. Instead of thousands of elements that include contact and frictional interfaces, the proposed method would feature a single element to represent the axial properties of a fastener (the method to incorporate shear properties is relegated to future work). Similar approaches have been proposed in the past (see (Coelho 2004) for an extensive literature review), including elastic-perfectly plastic models, bilinear models, and trilinear models (Sherbourne and Bahaari 1997). These models, generally, do not account of the softening behavior of a fastener observed prior to failure due to necking and other mechanisms.

There have been multiple efforts to study fasteners under failure in the literature. Most studies focus on larger assemblies rather than individual bolts (see, for instance, the review article (Dìaz et al. 2011)). It is worth noting that the model derived herein is general enough to accommodate these structures as well (at least in an axial sense), and that lessons learned from modeling the shear and rotational aspects of these structures can be applied to future work. Multiple experimental and numerical studies have been used to investigate the mechanics of a single fastener under axial loads, such as (Diegert et al. 1989; Lee et al. 2006; Segalman and Starr 2007; Ferjani, Averbuch, and Constantinescu 2011), which can provide a wealth of information for the present analysis. Much of the existing finite element analysis work for modeling of threaded fasteners has focused on two-dimensional or axisymmetric models (Assanelli and Dvorkin 1993; Segalman and Starr 2007; Ferjani, Averbuch, and Constantinescu 2011), which neglect the helix angle and three-dimensional effects of the fasteners, due to the prohibitive cost of having an adequately refined three-dimensional mesh. However, an alternative approach based on data mining and artificial intelligence algorithms to construct models that provide the most applicable solution for a given problem (Fernández et al. 2010) has shown some success in modeling the constitutive behavior of the fasteners. All of these approaches, it is worth noting, are significantly more advanced than the common practice found in most applications in which a linear spring is used to represent the jointed connection.

In what follows, the experimental results reported in the literature that are used in the present research are summarized in Section 2. From these experiments, a new elastic-plastic model of fastener failure is proposed in Section 3, which is then compared to approximately 100 experiments in the Appendix. The aim of the present model is to allow for an improved modeling of jointed connections in applications without significantly increasing the computational time (which would be necessary if high fidelity representations of the fasteners are used).

2 Summary of Existing Experiments

In order to develop a reduced order model for bolt force-displacement curves, experimental data from the Sandia Report (Lee et al. 2006) and the thesis (Wade 2006) are used. This data was digitized from the available PDF documents using the software DigitizeIt. An experiment matrix is presented in Table 1 for the experiments conducted in the Sandia reports and the results of these experiments are presented in Figs. 1-4. An experiment matrix for the experiments conducted in (Wade 2006) is provided in Table 2 and the data is provided in the Appendix.

A286 #8-32 UNC 5/8 in Length			
Gage Length [in]	Speed [in/s]	Preload [in.lb]	Washer
0.15	0.0002	0	No
0.15	2	0	No
0.25	0.0002	0	No
0.25	0.0002	20	No
0.25	1	20	No
0.25	1	20	Yes
0.25	2	0	No
AISI 8740 #8-32 UNC 5/8 in Length			
Gage Length [in]	Speed [in/s]	Preload [in.lb]	Washer
0.125	0.0002	0	No
0.28	0.0002	0	No
0.375	0.0002	0	No
A286 #10-32 UNF 5/8 in Length			
Gage Length [in]	Speed [in/s]	Preload [in.lb]	Washer
0.25	0.01	40	No
0.25	1	0	No
0.25	1	40	No
302HQ #10-32 UNF 5/8 in Length			
Gage Length [in]	Speed [in/s]	Preload [in.lb]	Washer
0.2	0.001	0	No
0.2	10	0	No
0.25	0.0002	0	No
0.25	2	0	No
0.375	0.0002	0	No
0.375	2	0	No

Table 1. Experiment matrix for test performed in (Lee et al. 2006).

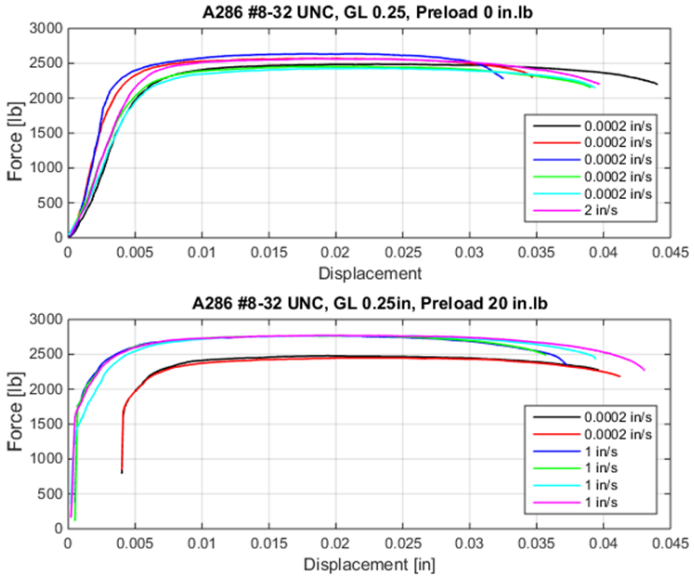

Figure 1. Tensile test results for A286 # 8-32 UNC separated based on preload.

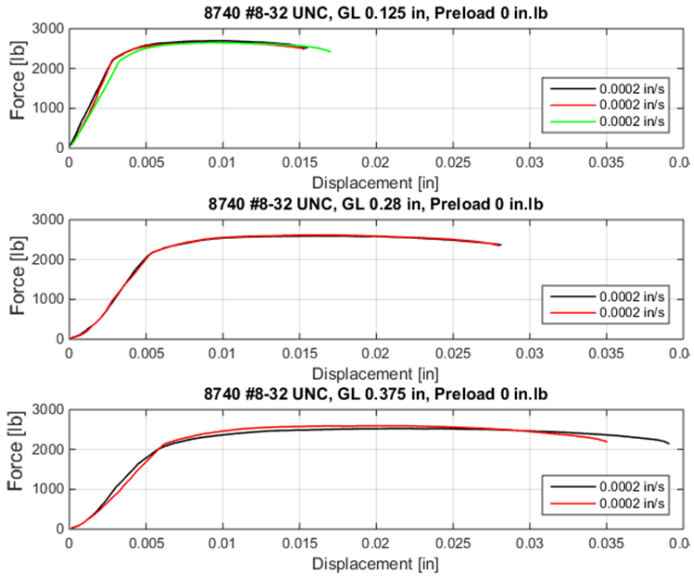

Figure 2. Tensile test results for AISI 8740 # 8-32 UNC separated based on gage length.

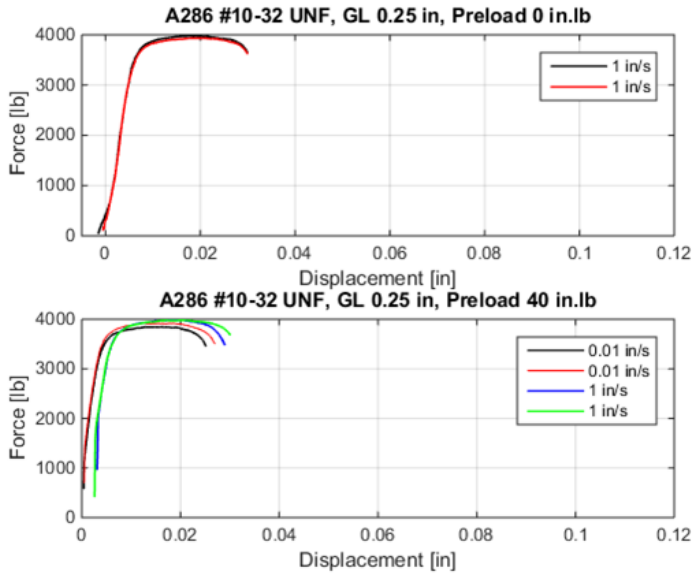

Figure 3. Tensile test results for A286 # 10-32 UNF separated based on gage length.

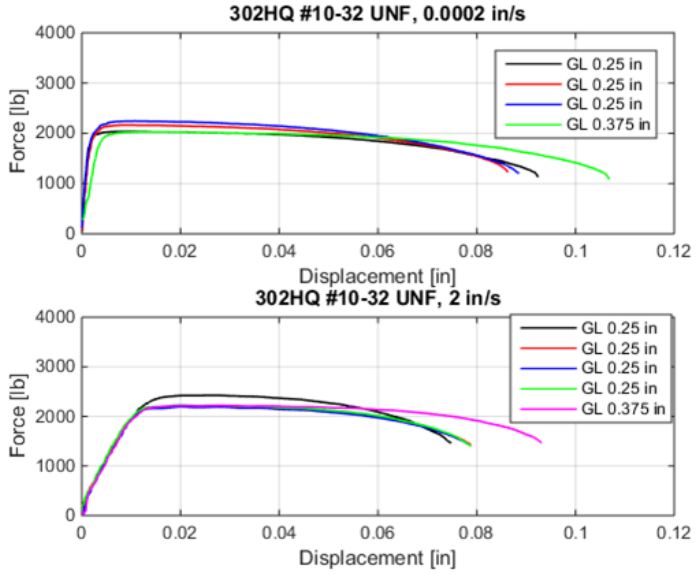

Figure 4. Tensile test results for 302HQ # 10-32 UNF separated based on displacement rate.

A325 3/4-10 UNC	**A325 1-8 UNC**	**A490 3/4-10 UNC**	**A490 1 1/4-7 UNC**
Gage Length [in]	Gage Length [in]	Gage Length [in]	Gage Length [in]
0.6	0.8	0.6	3.5
0.75	0.9	0.8	3.95
0.8	1.2	1.0	4.5
1.0	2.4	1.2	
1.2		1.95	

Table 2. Experiment matrix for test performed in (Wade 2006)

3 Model Development

Multiple approaches were investigated in the development of the present model, including the Ramberg-Osgood model (Dìaz et al. 2011). However, these approaches were found to be unable to represent accurately the constitutive behavior of the fastener as compared to the empirical model proposed in what follows.

Given that the typical stress strain behavior of a metal is to start off in an initial linear (elastic) region that quickly grows and transitions into a nonlinear (plastic) region, this relationship is modeled as the superposition of an elastic function and a plastic function (similar to the contact modeling in (Brake 2015))

$$\sigma(\varepsilon) = \Phi_1(\varepsilon)\sigma_{elastic} + \Phi_2(\varepsilon)\sigma_{plastic}, \tag{1}$$

where $\Phi_1(\varepsilon)$ and $\Phi_2(\varepsilon)$ are any general functions of ε that can be linear or nonlinear, $\sigma_{elastic}$ is the characteristic elastic stress comparable to a yield stress, and $\sigma_{plastic}$ is the characteristic plastic stress comparable to the ultimate stress. Analogous to this, the force displacement relationship is

$$F(\delta) = \phi_1(\delta)F_{elastic} + \phi_2(\delta)F_{plastic} \tag{2}$$

with general functions $\phi_1(\delta)$ and $\phi_2(\delta)$ of displacement δ that can be linear or nonlinear. The force $F_{elastic}$ is the characteristic elastic force comparable to a yield force, and $F_{plastic}$ is the characteristic plastic force comparable to the ultimate force. The task is, therefore, to identify the appropriate functions $\phi_1(\delta)$ and $\phi_2(\delta)$, which can depend on the material, geometry, loading, etc. While this functional form is applicable broadly, this report specifically develops and applies it to the force-displacement relationship for a bolt.

Extending the plastic region to the origin, as in Fig. 5, the area between the actual curve and the extended curve resembles an upside down and slightly rotated Gaussian distribution. Furthermore, if the plastic curve was extended beyond the origin, it would also resemble a Gaussian distribution approximately centered about the peak displacement. This result, therefore, leads to the choice of two Gaussian distribution functions for $\phi_1(\delta)$ and $\phi_2(\delta)$

$$\phi_1(\delta) = -exp\left(-\left(\frac{\delta}{\delta_{el}}\right)^2\right), \;\; \phi_2(\delta) = \exp\left(-\left(\frac{\delta-\delta_{pl1}}{\delta_{pl2}}\right)^2\right) \tag{3}$$

Substituting Eq. 3 into Eq. 2,

$$F(\delta) = -F_{el}\exp\left(-\left(\frac{\delta}{\delta_{el}}\right)^2\right) + F_{pl}\exp\left(-\left(\frac{\delta-\delta_{pl1}}{\delta_{pl2}}\right)^2\right) \tag{4}$$

This functional form has five parameters δ_{el}, δ_{pl1}, δ_{pl2}, F_{el}, and F_{pl} that will be determined in the following discussion and analysis.

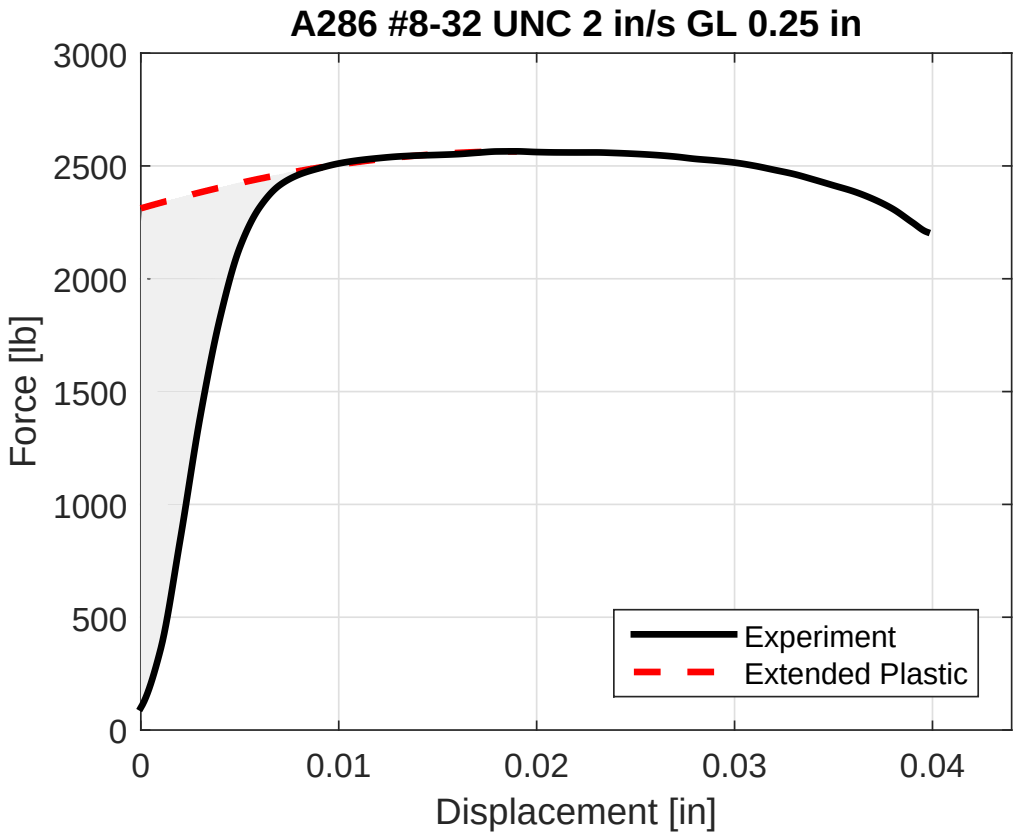

Figure 5. Typical force displacement curve with plastic curve extended to the y axis.

3.1 Elimination of Free Parameters

Two parameters, F_{pl} and δ_{pl1}, are identified immediately as the maximum force in the plastic region must be the peak force and that the distribution should be centered about the peak displacement. Thus,

$$F_{pl} \equiv F_p, \quad \delta_{pl1} \equiv \delta_p \tag{5}$$

This relationship reduces the total number of free parameters from five to three with two experimentally measured parameters.

Since the plastic portion spans a greater extent than the elastic portion, it is expected that $\delta_{pl2} >> \delta_{el}$. Furthermore, due to the curvature of the plastic portion, it is concluded that the standard deviation of the plastic Gaussian distribution function must be larger than the fracture displacement, δ_f. To this end, δ_{pl2} is defined via

$$\delta_{pl2} \equiv \delta_p + \delta_f. \tag{6}$$

For the elastic portion, the majority of the elastic displacement δ_{el} must occur before the elastic

limit or a prototypical yield displacement. Thus, $\delta_{el} \neq \delta_y$, and is given in the model as

$$\delta_{el} = \beta \delta_y, \;\; 0 < \beta < 1 \tag{7}$$

for a yet to be determined scaling constant β. Finally, since the yield force occurs at the transition between elastic and plastic regimes, it is assumed that

$$F_{el} \approx F_y. \tag{8}$$

Substituting Eqs. 5-8 into Eq. 4 and letting $\alpha = 1/\beta$, the intermediate form of the constitutive model is

$$F(\delta) = -F_y \exp\left(-\left(\alpha \frac{\delta}{\delta_y}\right)^2\right) + F_p \exp\left(-\left(\frac{\delta - \delta_p}{\delta_p + \delta_f}\right)^2\right), \tag{9}$$

where the free parameters are F_y and α, and δ_y is the displacement associated with F_y. It is not always possible to determine the exact yield force and displacement, so F_y is left as a free parameter for now.

To fit the free parameters, an optimization study is employed to understand the situation in which the correlation between the model and ten experiments (the R^2 value) is maximzed for A286 #8-32 UNC bolts. The results of this optimization are presented in Table 3.

A286 #8-32 UNC 5/8 in Length						
Gage Length [in]	Speed [in/s]	R^2	α	F_y	F_p	F_y/F_p
0.15	0.0002	0.9992	1.50	2163	2553	0.85
0.25	0.0002	0.9990	1.46	2027	2460	0.82
0.25	0.0002	0.9990	1.55	2108	2487	0.85
0.25	0.0002	0.9979	1.52	2114	2570	0.82
0.25	0.0002	0.9967	1.61	2230	2636	0.85
0.25	0.0002	0.9992	1.38	1952	2428	0.80
0.25	0.0002	0.9987	1.38	1961	2456	0.80
0.15	2	0.9973	1.36	2267	2663	0.85
0.25	2	0.9986	1.37	2107	2571	0.82
0.25	2	0.9988	1.45	2139	2565	0.83
Mean			**1.46**	**2107**	**2539**	**0.82**

Table 3. Initial optimization study for A286 8-32 UNC bolts.

The values of $\alpha^{-1} \approx F_y/F_p$, prompting the approximation

$$F_y \approx \frac{1}{\alpha} F_p. \tag{10}$$

With the reduction in free parameters from Eq. 10, a second optimization study yields that $\alpha \approx 1.25$, as seen in Table 3.2.

A286 #8-32 UNC 5/8 in Length						
Gage Length [in]	Speed [in/s]	R^2	α	F_y	F_p	F_y/F_p
0.15	0.0002	0.9963	1.26	2022	2553	0.79
0.25	0.0002	0.9973	1.27	1937	2460	0.79
0.25	0.0002	0.9955	1.27	1961	2487	0.79
0.25	0.0002	0.9953	1.28	2005	2570	0.78
0.25	0.0002	0.9937	1.27	2079	2636	0.79
0.25	0.0002	0.9981	1.27	1905	2428	0.78
0.25	0.0002	0.9975	1.28	1920	2456	0.78
0.15	2	0.9954	1.23	2158	2663	0.81
0.25	2	0.9978	1.26	2037	2571	0.79
0.25	2	0.9968	1.26	2028	2565	0.79
Mean			**1.27**	**2005**	**2539**	**0.79**

Table 4. Second optimization study for A286 8-32 UNC bolts.

3.2 The Fixed Parameter Form

From the two optimization studies, all free parameters have been removed from the model, leaving only experimentally measured values. This yields the functional form of the constitutive model

$$F(\delta) = F_p \left[\frac{4}{5} \exp\left(-\left(\frac{5}{4} \frac{\delta}{\delta_{80}} \right)^2 \right) + \exp\left(-\left(\frac{\delta - \delta_p}{\delta_p + \delta_f} \right)^2 \right) \right] \tag{11}$$

Note that this is based on the displacement δ_{80} associated with the force $0.8F_p$ and $\delta_{80} < \delta_p$, both of which are experimentally measured.

Thus, the original model (Eq. 4), which consisted of five free parameters, is reduced to a form with zero free (tunable) parameters without sacrificing the simplicity of the original form. The cost of this reduction is the necessity of additional measured data points, resulting in the final model depending on four measured parameters: $\{F_p, \delta_{80}, \delta_p, \delta_f\}$. This model form is valid for high strength, low ductility fasteners, however, it does not work well for high ductility, lower strength fasteners especially materials that are strain rate dependent. The model results for A286, AISI 8740, A325, and A490 bolts are presented in Appendix A.

3.3 The Generalized Model

In particular, the model of Eq. 11 does not model accurately the force displacement curves for 302HQ bolts at low strain rates. If the exponent in the plastic Gaussian distribution function is

A286 #8-32 UNC 5/8 in Length						
Gage Length [in]	Speed [in/s]	R^2	α	F_y	F_p	F_y/F_p
0.15	0.0002	0.9957	1.25	2042	2553	0.80
0.25	0.0002	0.9930	1.25	1968	2460	0.80
0.25	0.0002	0.9951	1.25	1989	2487	0.80
0.25	0.0002	0.9920	1.25	2056	2570	0.80
0.25	0.0002	0.9899	1.25	2108	2636	0.80
0.25	0.0002	0.9939	1.25	1942	2428	0.80
0.25	0.0002	0.9951	1.25	1965	2456	0.80
0.15	2	0.9944	1.25	2130	2663	0.80
0.25	2	0.9959	1.25	2056	2571	0.80
0.25	2	0.9971	1.25	2052	2565	0.80
Mean			**1.25**	**2031**	**2539**	**0.80**

Table 5. Results for final model of A286 8-32 UNC bolts.

changed from two to three such that the model becomes

$$F(\delta) = F_p \left[\frac{4}{5} \exp\left(-\left(\frac{5}{4} \frac{\delta}{\delta_{80}} \right)^2 \right) + \exp\left(-\left(\frac{\delta - \delta_p}{\delta_p + \delta_f} \right)^3 \right) \right], \tag{12}$$

the resulting model better predicts the behavior of high ductility steels. Equation 12 is used to model the force displacement curves for 302HQ bolts for displacement rates of 0.001 in/s and 0.0002 in/s, whereas Eq. 11 is used for displacement rates of 2 in/s and 10 in/s. More data is needed to understand the transition between these two strain rates, but a functional form spanning both of them might be

$$F(\delta) = F_p \left[\frac{4}{5} \exp\left(-\left(\frac{5}{4} \frac{\delta}{\delta_{80}} \right)^2 \right) + \exp\left(-\left(\frac{\delta - \delta_p}{\delta_p + \delta_f} \right)^{2+\chi(v)} \right) \right], \tag{13}$$

$$\chi(v) = \tanh(10 \mid v \mid) \tag{14}$$

in which v is the experimental loading rate and the constant 10 is for scaling purposes. Empirically, χ is similar to the power law hardening index n (related to the Meyer's hardness exponent as $2+n$): for values of $n = 0$, no work hardening is expected in a material, and $n = 1$ is an upper bound that is generally observed.

The results for 302HQ fasteners are presented in Appendix B with the results using Eq. 11 for low displacement rates first followed by the results using Eq. 13 for low displacement rates. The results using Eq. 13 for high displacement rates are then presented.

4 Summary and Conclusions

A new, four-parameter fastener failure model is developed for bolts in tension. The four parameters

F_p Maximum force in loading

δ_p Displacement at F_p

δ_{80} Displacement at $0.80 \times F_p$

δ_f Displacement at failure

are all taken from measurements of a representative bolt. The final functional form is thus given as

$$F(\delta) = F_p \left[\frac{4}{5} \exp\left(-\left(\frac{5}{4} \frac{\delta}{\delta_{80}} \right)^2 \right) + \exp\left(-\left(\frac{\delta - \delta_p}{\delta_p + \delta_f} \right)^{2+\chi(v)} \right) \right], \tag{15}$$

$$\chi(v) = \tanh(10 \mid v \mid). \tag{16}$$

Future work is needed to improve the form of $\chi(v)$ as it has not been rigorously derived.

This single degree of freedom constitutive model has the capability of reproducing force displacement curves with high accuracy, and it is based on observations of the shape of measured curves. The model was reduced from having five free parameters down to zero free parameters; however, the resulting model is entirely empirical and requires four experimentally measured parameters. Of these parameters, the peak force F_p (ultimate stress) is generally reported for bolts whereas the necessary displacements, with the exception of the displacement at 80% of the peak force, can be difficult to determine without experiment.

Future work on this project involves identifying additional shape functions, extending the model for specimens loaded in shear, and developing parameters to estimate the necessary displacements without the need for experiment. An additional investigation into the effect of test setup on the force displacement curves for a given bolt may also be necessary.

References

Assanelli, A. P. and E. N. Dvorkin (1993). “Finite Element Models of OCTG Threaded Connections”. In: *Computers and Structures* 47, pp. 725–734.

Brake, M. R. W. (2015). “An Analytical Elastic Plastic Contact Model with Strain Hardening and Frictional Effects for Normal and Oblique Impacts”. In: *International Journal of Solids and Structures* 62, pp. 104–123.

Coelho, A. M. G. (2004). *Characterization of the Ductility of Bolted End Plate Beam-to-Column Steel Connections*. Doctoral Dissertation. Universidade de Coimbra, Coimbra, Portugal.

Dìaz, C. et al. (2011). “Review on the Modelling of Joint Behaviour in Steel Frames”. In: *Journal of Constructional Steel Research* 67, pp. 741–758.

Diegert, K. V. et al. (1989). *Small Screw Study - Interim Report on Fastener Tensile Strength and Optimum Thread Depth*. SAND89-1320. Sandia National Laboratories, Albuquerque, NM.

Ferjani, M., D. Averbuch, and A. Constantinescu (2011). “A Computational Approach for the Fatigue Design of Threaded Connections”. In: *International Journal of Fatigue* 33, pp. 610–623.

Fernández, J. et al. (2010). “Prediction Models for Calculating Bolted Connections Using Data Mining Techniques and the Finite Element Method”. In: *Engineering Structures* 32, pp. 3018–3027.

Ju, S.-H., C.-Y. Fan, and G. H. Wu (2004). “Three-Dimensional Finite Elements of Steel Bolted Connections”. In: *Engineering Structures* 26, pp. 403–413.

Kim, J., J.-C. Yoon, and B.-S. Kang (2007). “Finite Element Analysis and Modeling of Structure with Bolted Joints”. In: *Applied Mathematical Modelling* 31, pp. 895–911.

Lee, S. et al. (2006). *Experimental Results of Single Screw Mechanical Tests: A Follow-Up to SAND2005-6036*. SAND2006-3751. Sandia National Laboratories, Livermore, CA.

Segalman, D. J. and M. J. Starr (2007). “Modeling of Threaded Joints Using Anisotropic Elastic Continua”. In: *ASME Journal of Applied Mechanics* 74, pp. 575–585.

Sherbourne, A. N. and M. R. Bahaari (1997). “Finite Element Prediction of End Plate Bolted Connection Behavior. I: Parametric Study”. In: *ASCE Journal of Structural Engineering* 123, pp. 157–164.

Wade, Patrick M. (2006). “Characterization of High-Strength Bolt Behavior in Bolted Moment Connections”. MSc. North Carolina State University.

A Appendix: High Strength Model Results

A.1 A286 Results

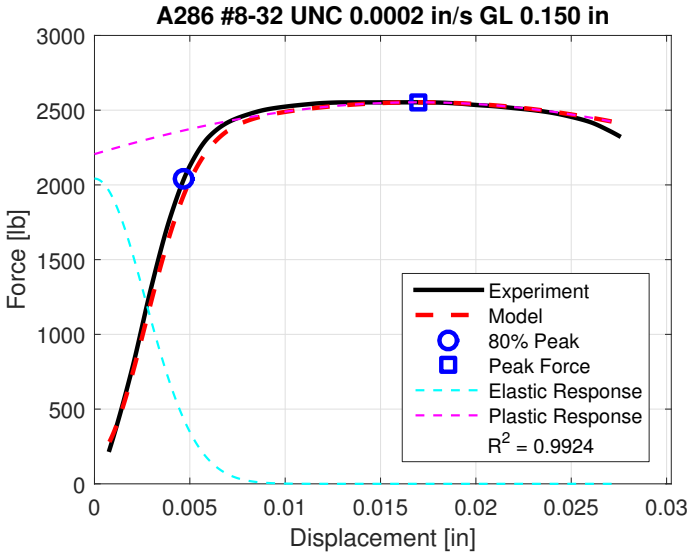

Figure A.1.

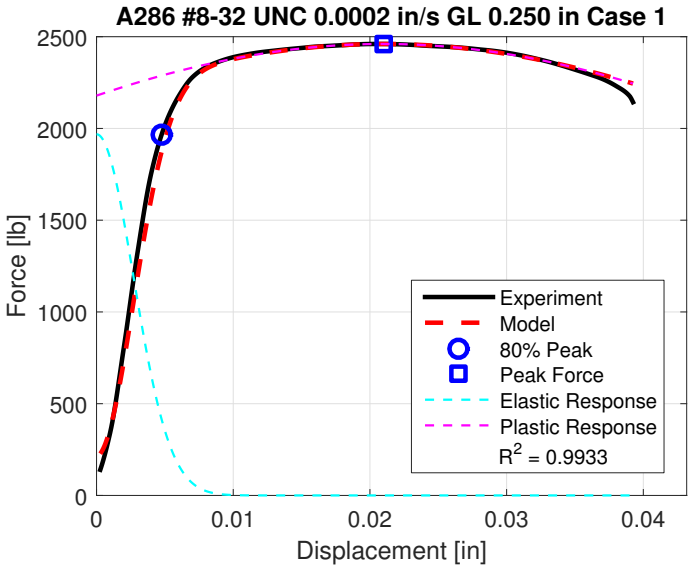

Figure A.2.

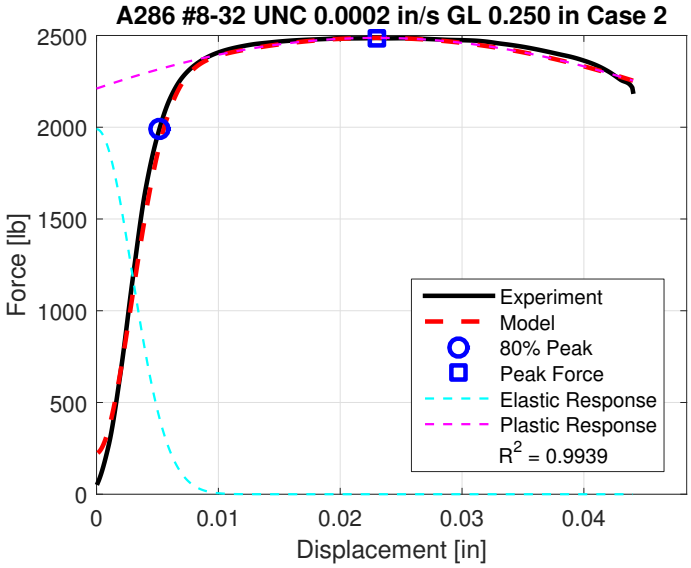

Figure A.3.

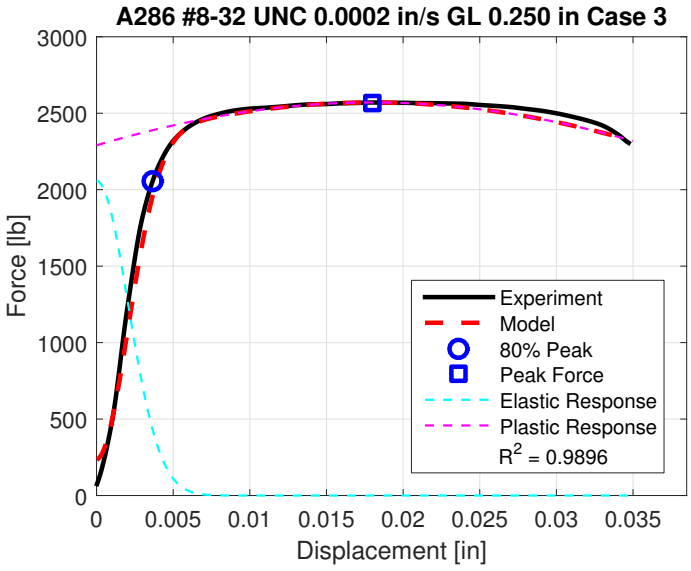

Figure A.4.

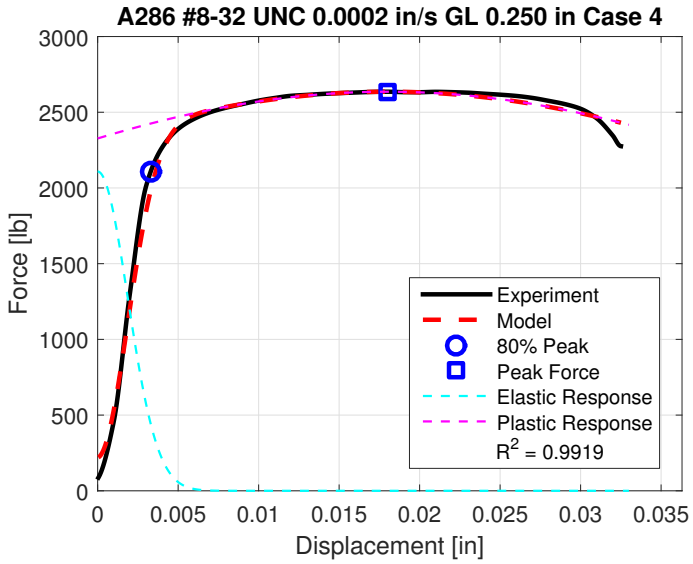

Figure A.5.

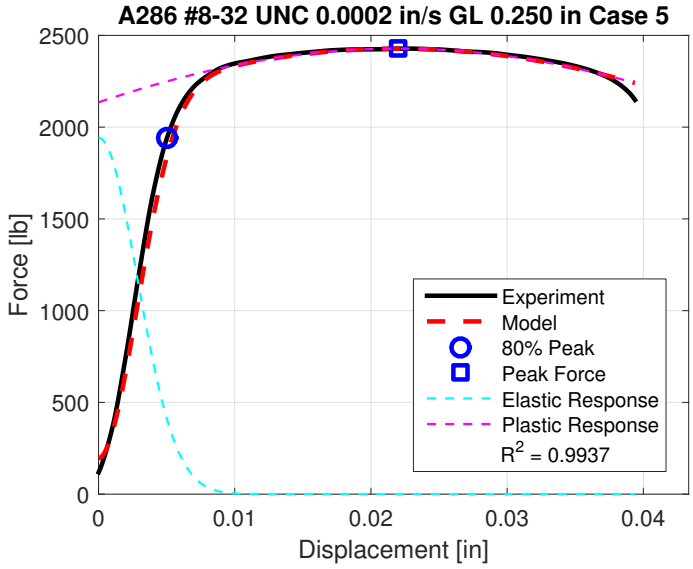

Figure A.6.

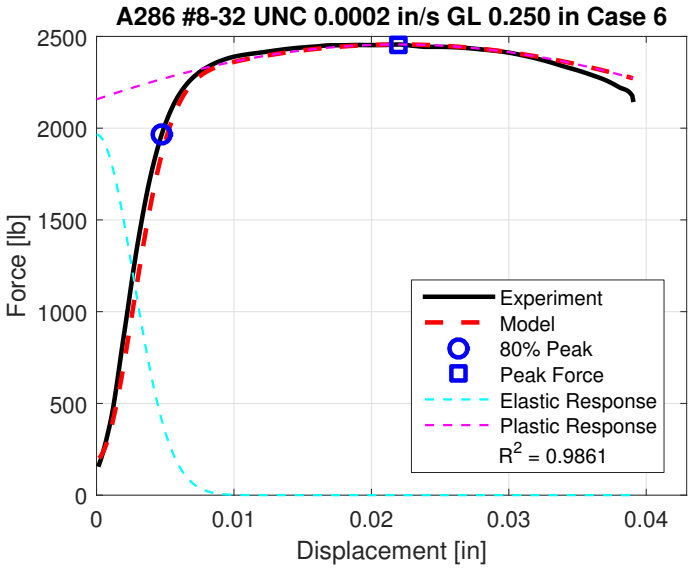

Figure A.7.

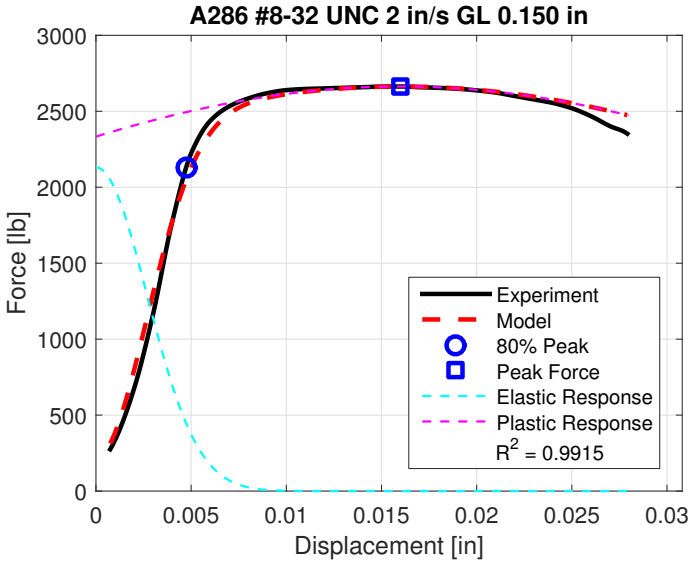

Figure A.8.

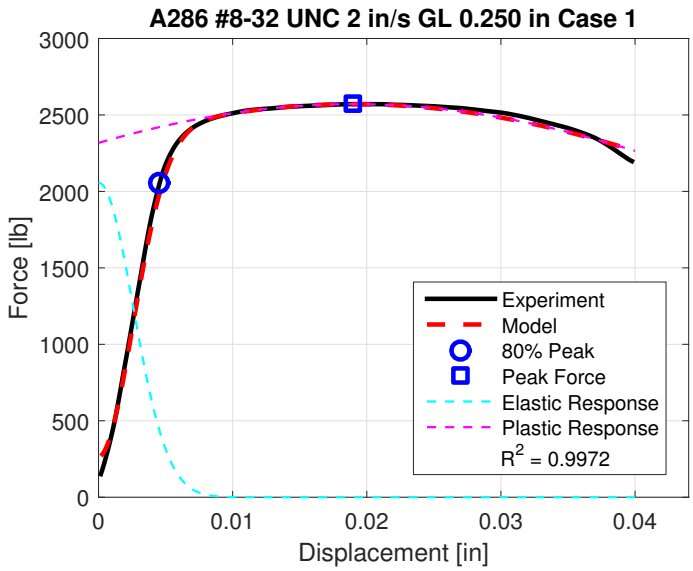

Figure A.9.

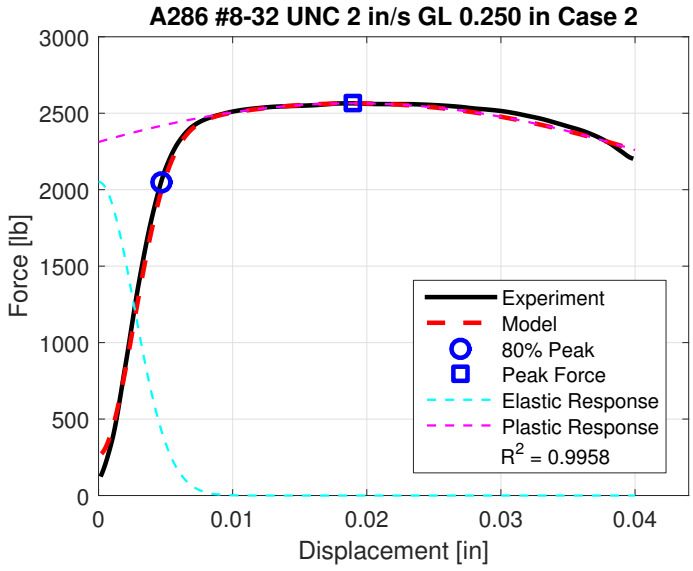

Figure A.10.

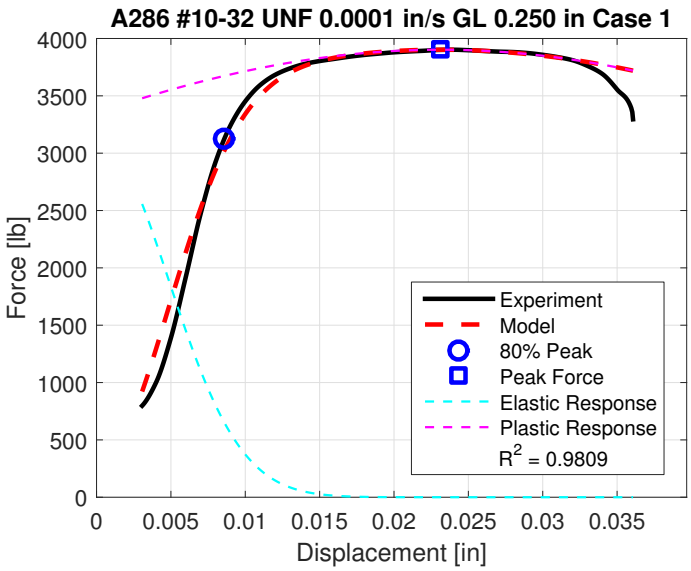

Figure A.11.

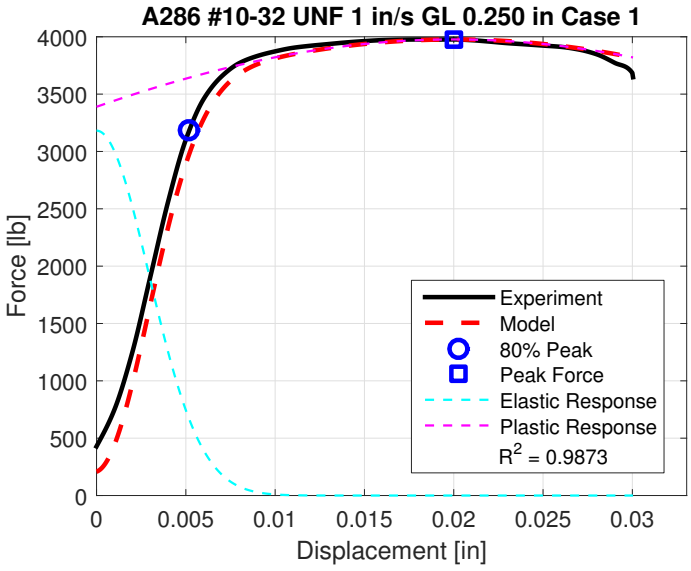

Figure A.12.

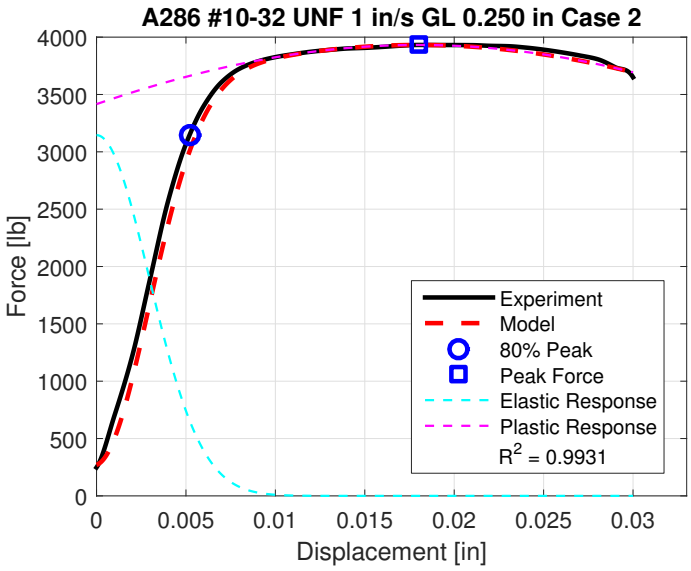
A286 #10-32 UNF 1 in/s GL 0.250 in Case 2
Force [lb]
Displacement [in]
0
500
1000
1500
2000
2500
3000
3500
4000
0
0.005
0.01
0.015
0.02
0.025
0.03
Experiment
Model
80% Peak
Peak Force
Elastic Response
Plastic Response
R2 = 0.9931

Figure A.13.

A.2 AISI 8740 Results

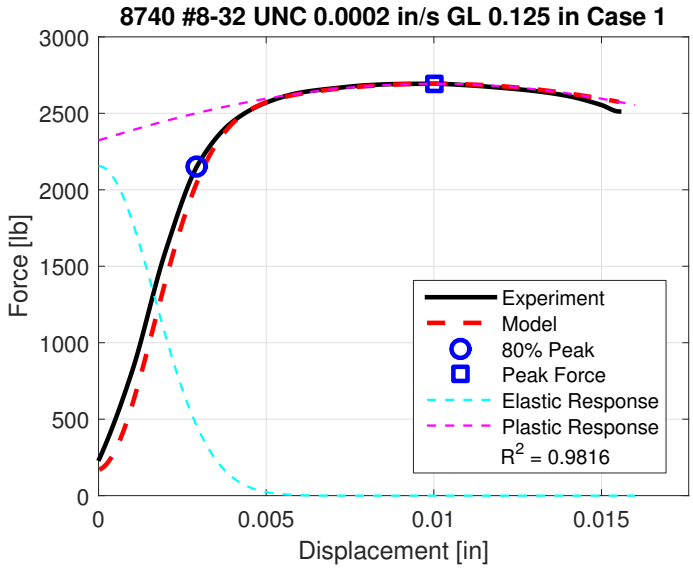

Figure A.14.

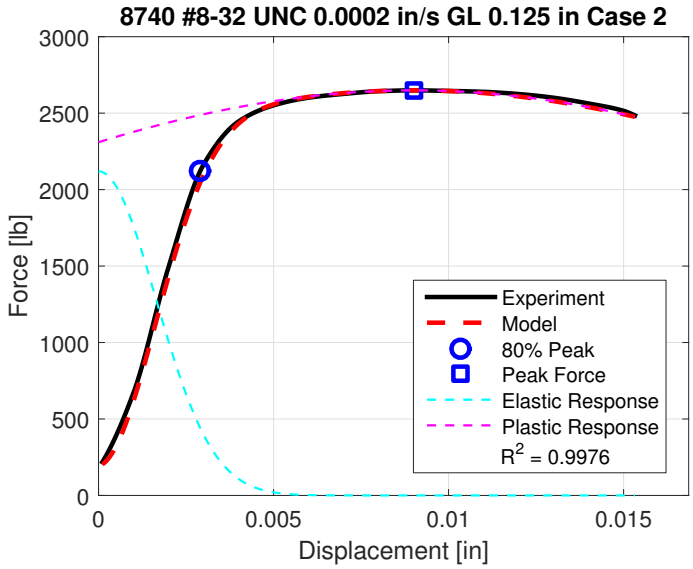

Figure A.15.

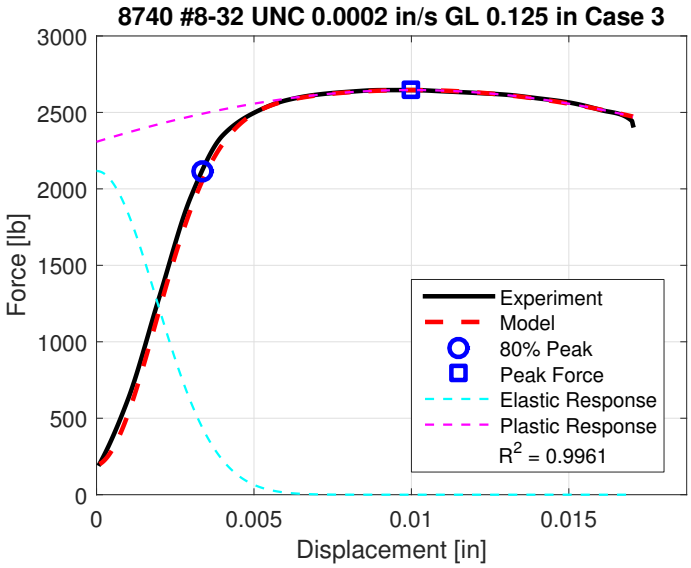

Figure A.16.

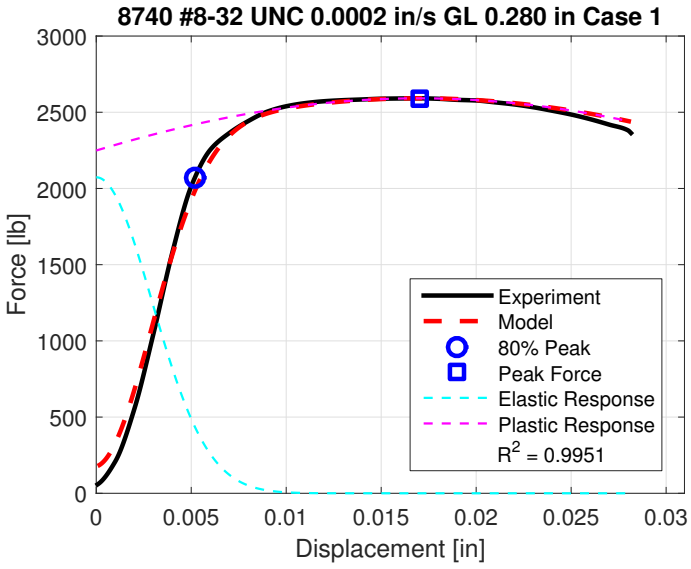

Figure A.17.

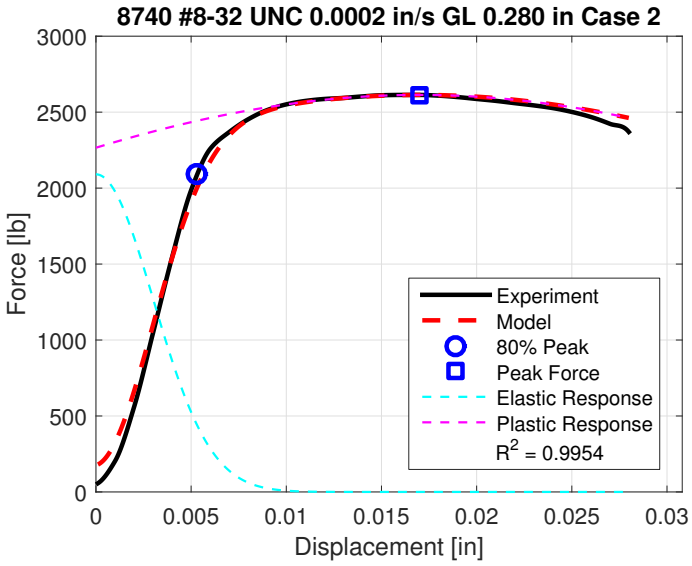

Figure A.18.

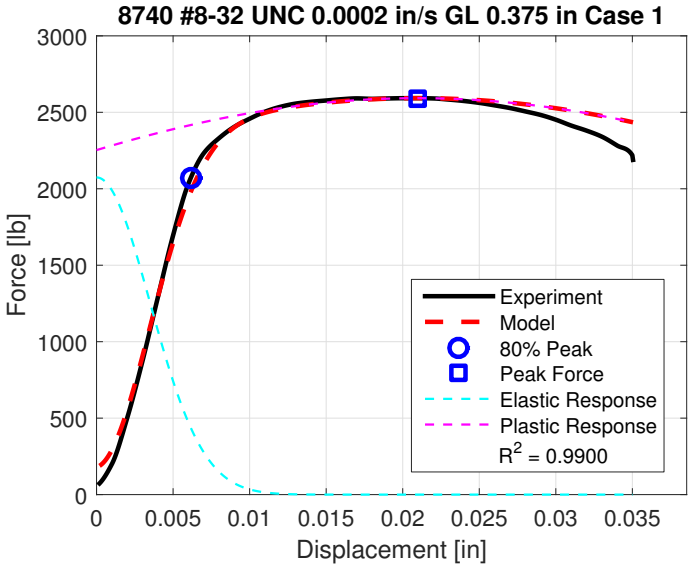

Figure A.19.

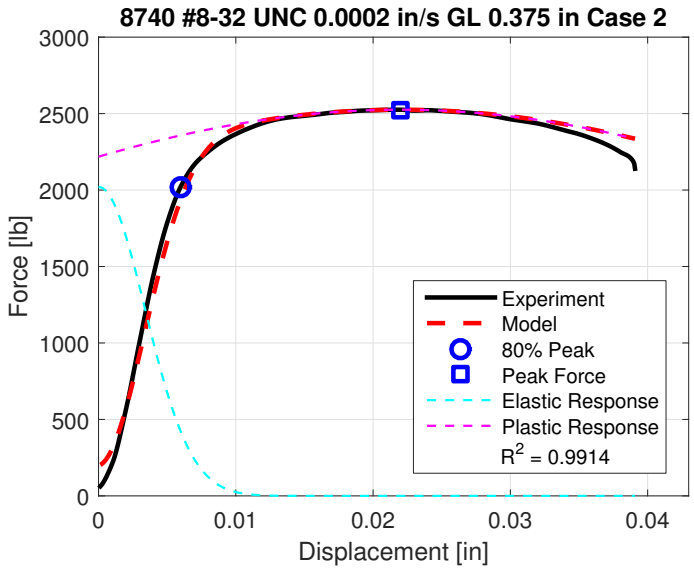
8740 #8-32 UNC 0.0002 in/s GL 0.375 in Case 2
Force [lb]
Displacement [in]
3000
2500
2000
1500
1000
500
0
0
0.01
0.02
0.03
0.04
Experiment
Model
80% Peak
Peak Force
Elastic Response
Plastic Response
R2 = 0.9914

Figure A.20.

A.3 A325 Results

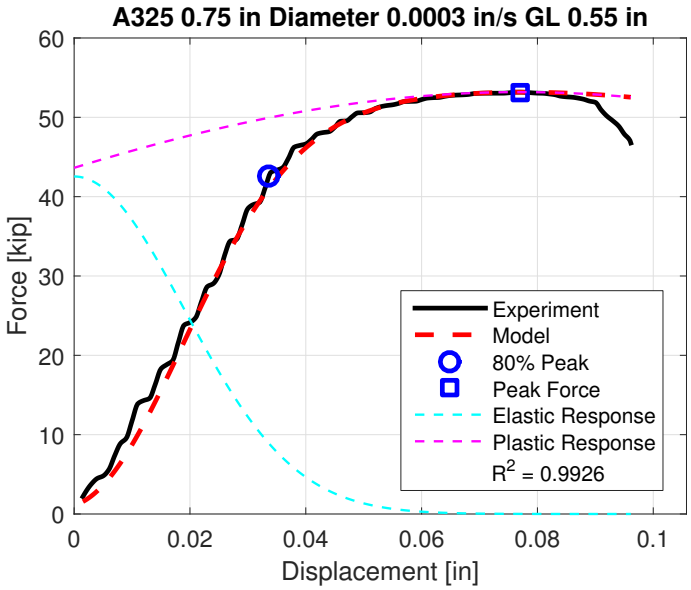

Figure A.21.

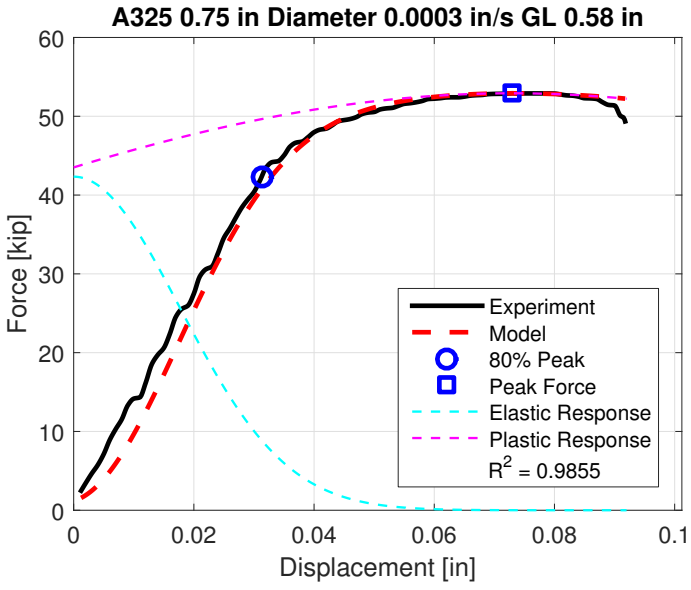

Figure A.22.

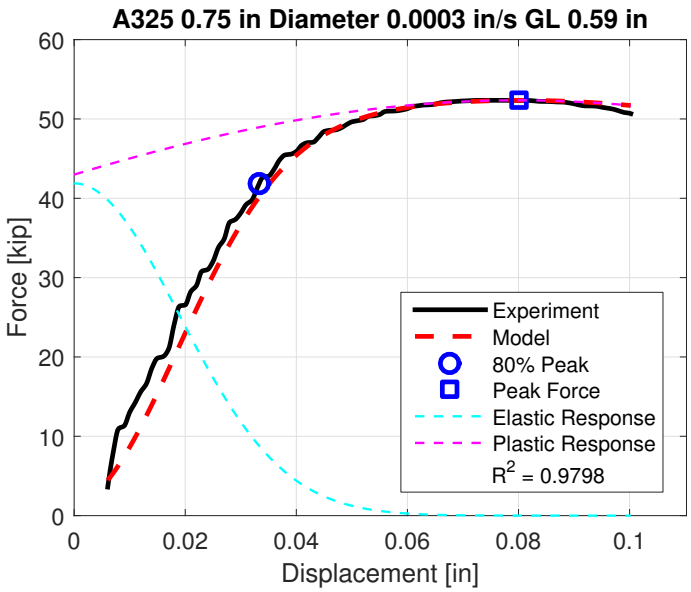

Figure A.23.

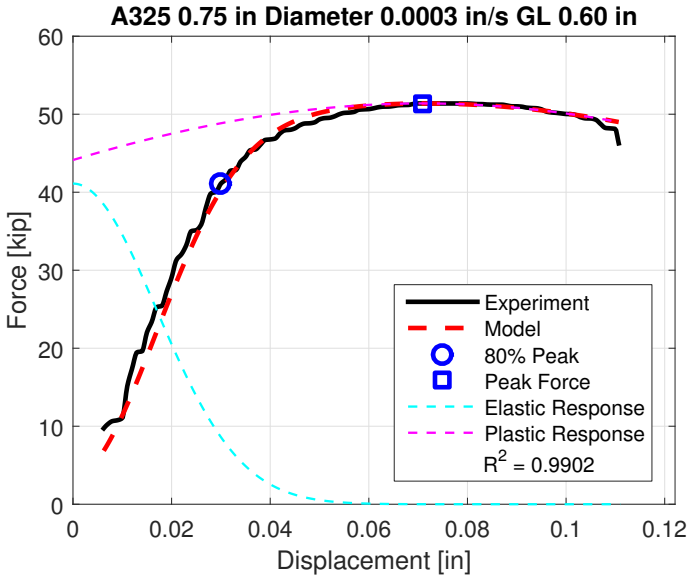

Figure A.24.

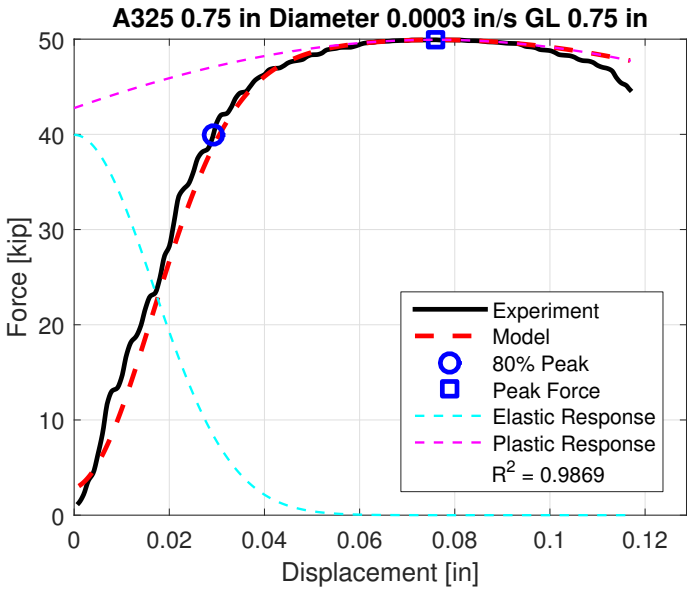

Figure A.25.

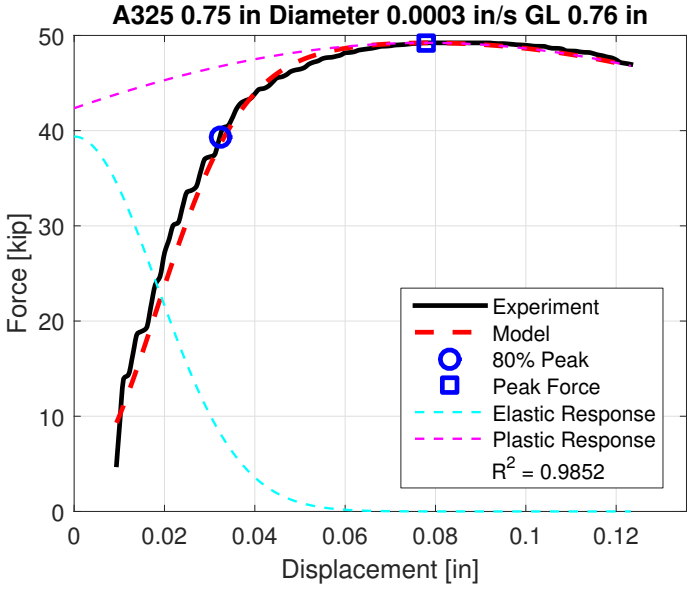

Figure A.26.

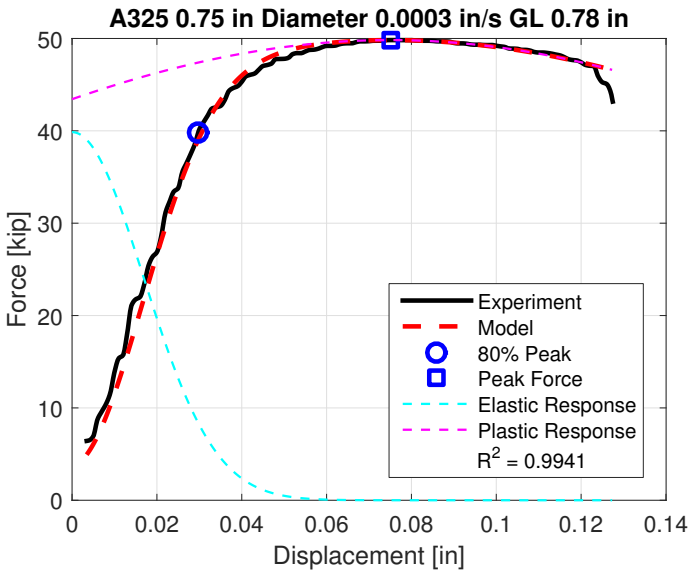

Figure A.27.

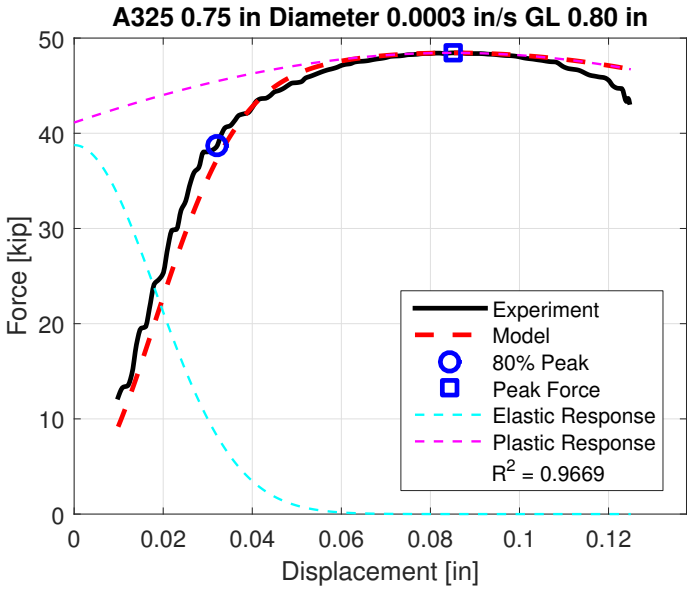

Figure A.28.

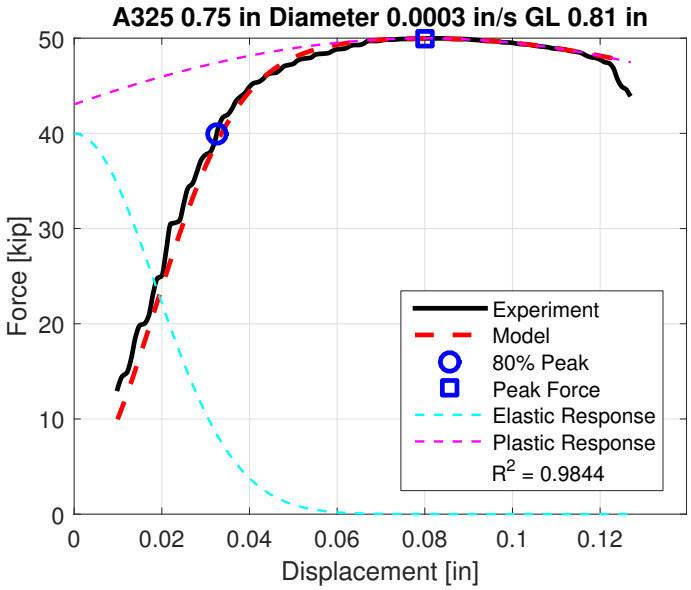

Figure A.29.

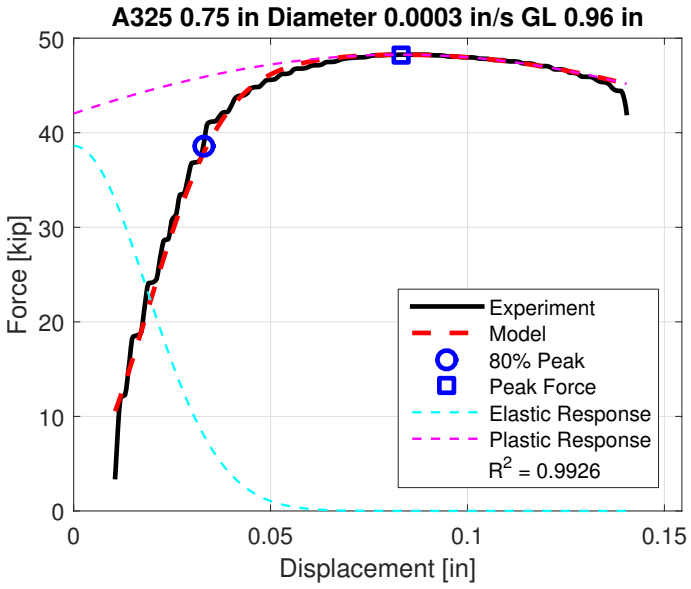

Figure A.30.

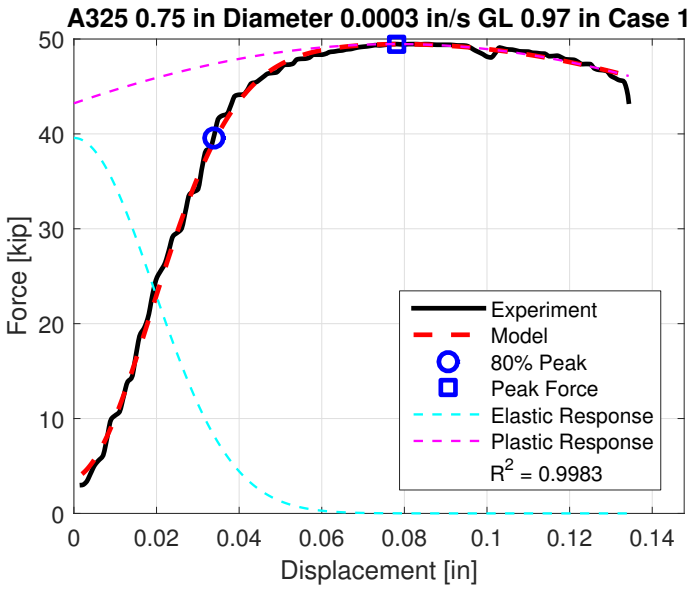

Figure A.31.

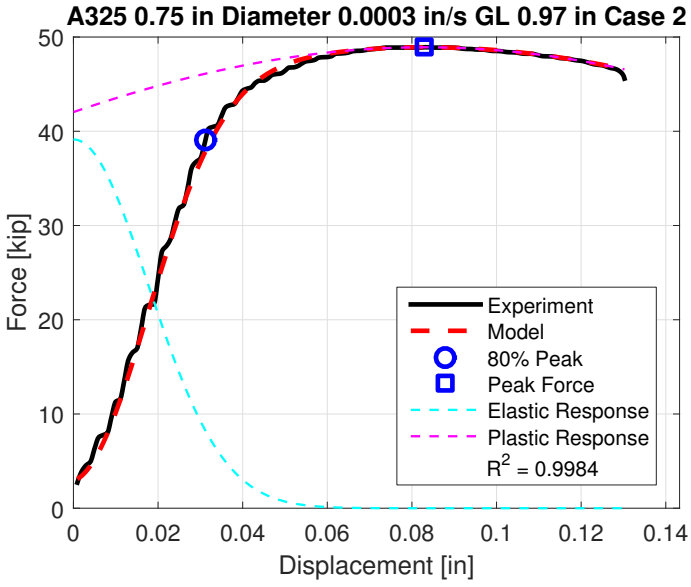

Figure A.32.

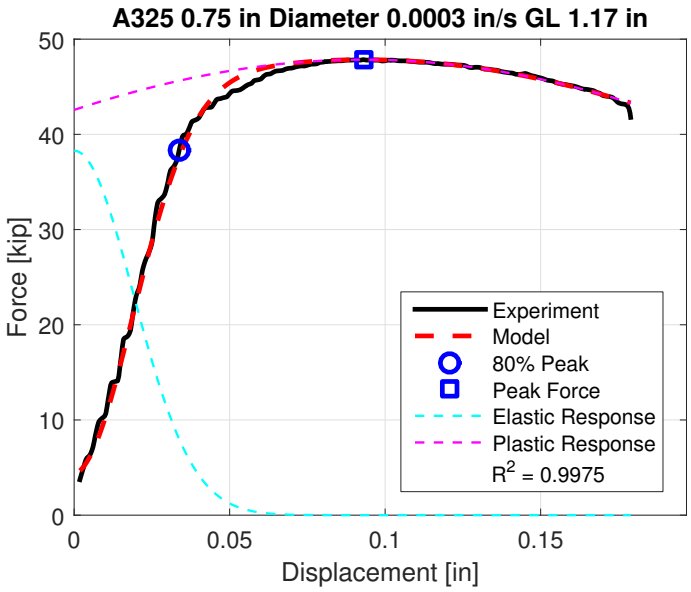

Figure A.33.

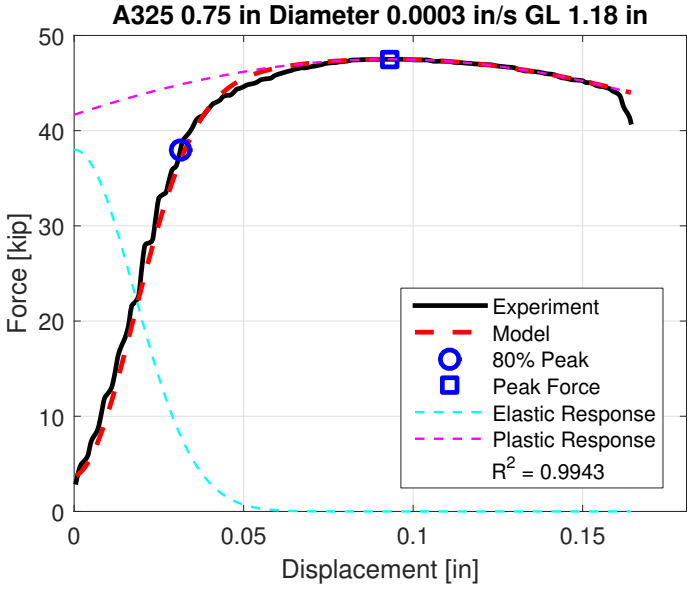

Figure A.34.

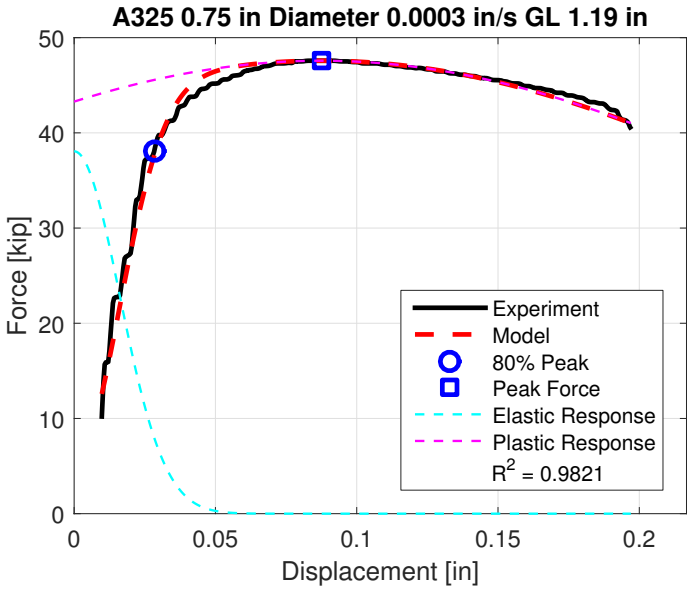

Figure A.35.

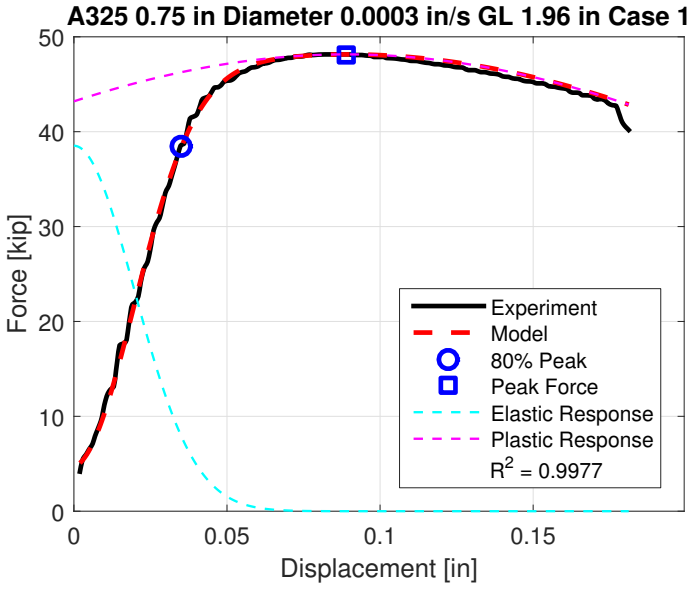

Figure A.36.

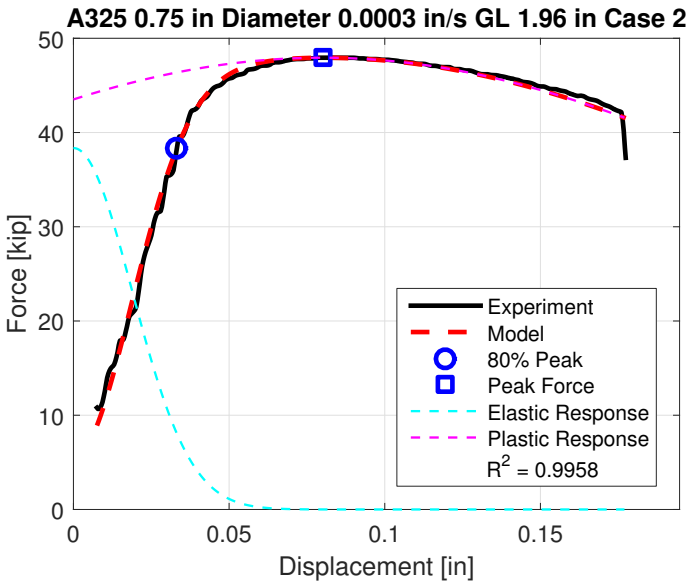

Figure A.37.

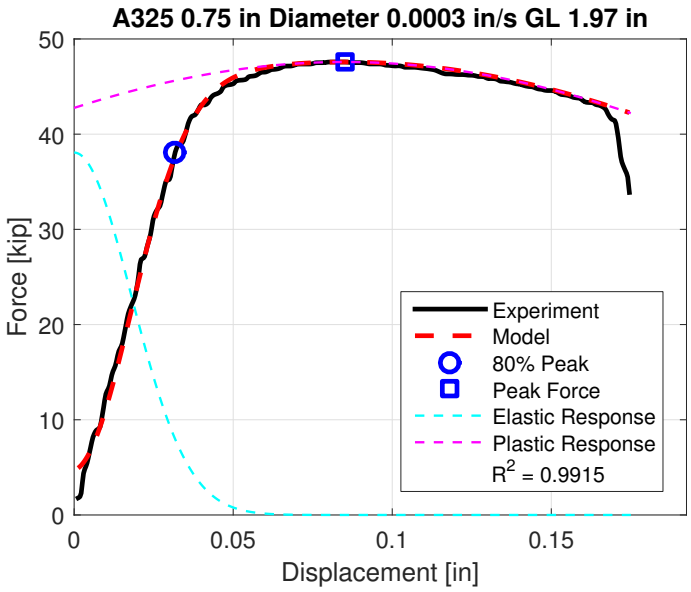

Figure A.38.

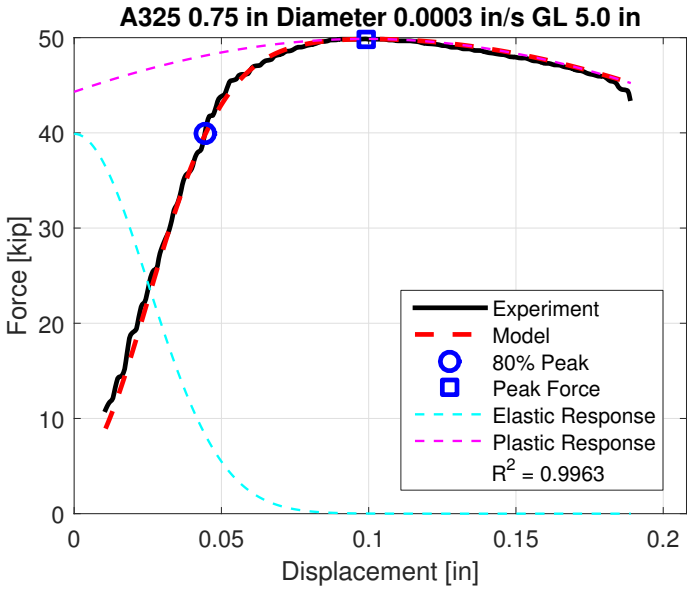

Figure A.39.

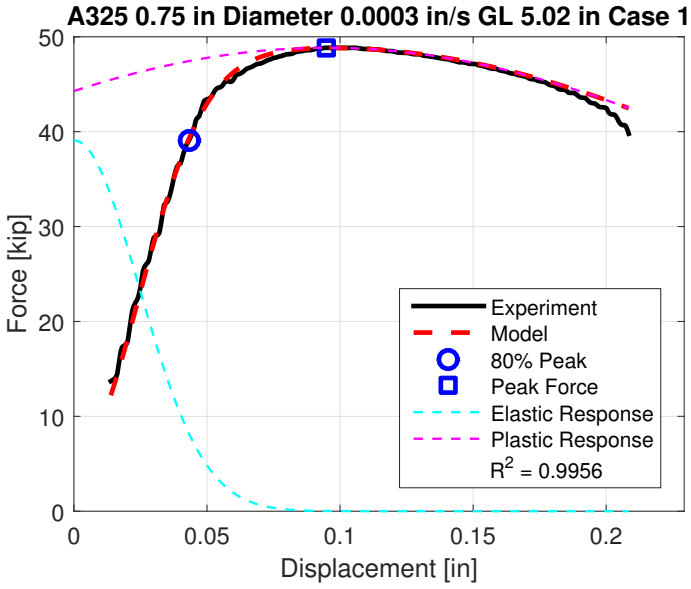

Figure A.40.

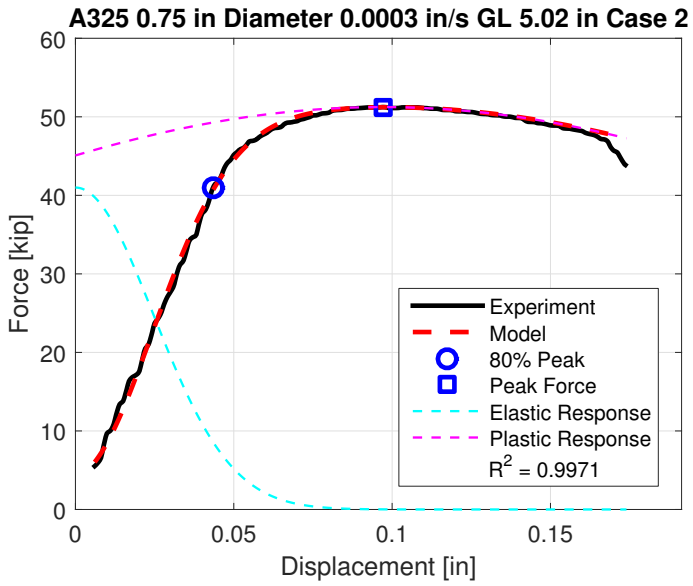

Figure A.41.

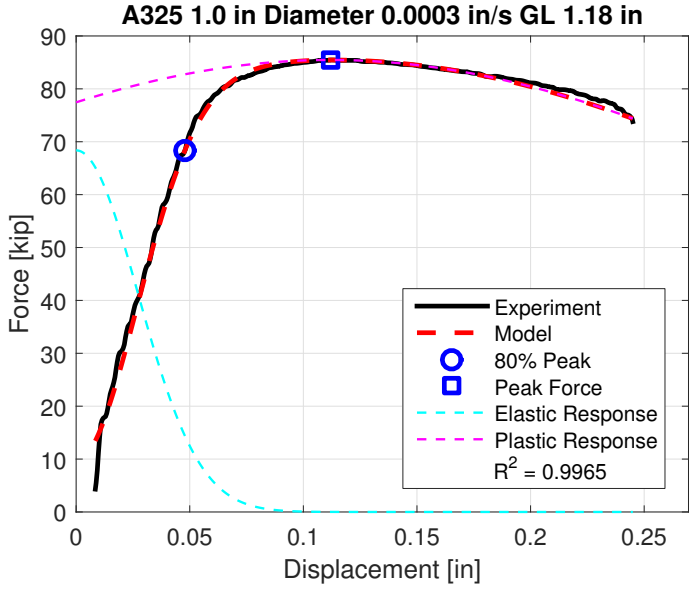

Figure A.42.

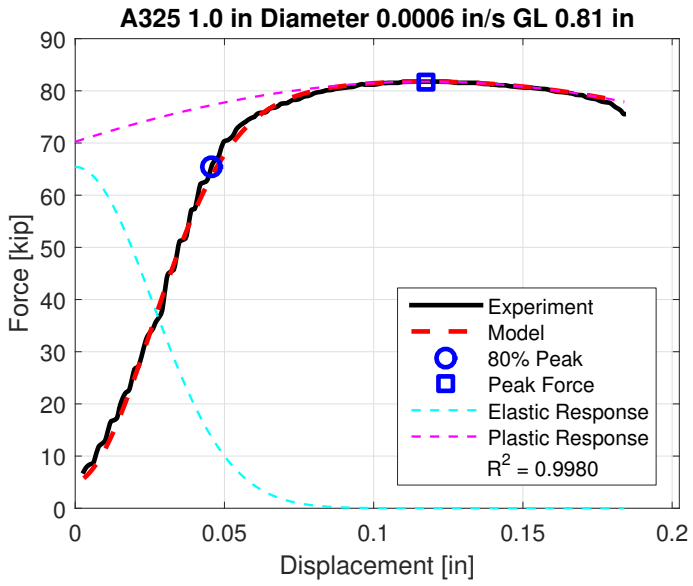

Figure A.43.

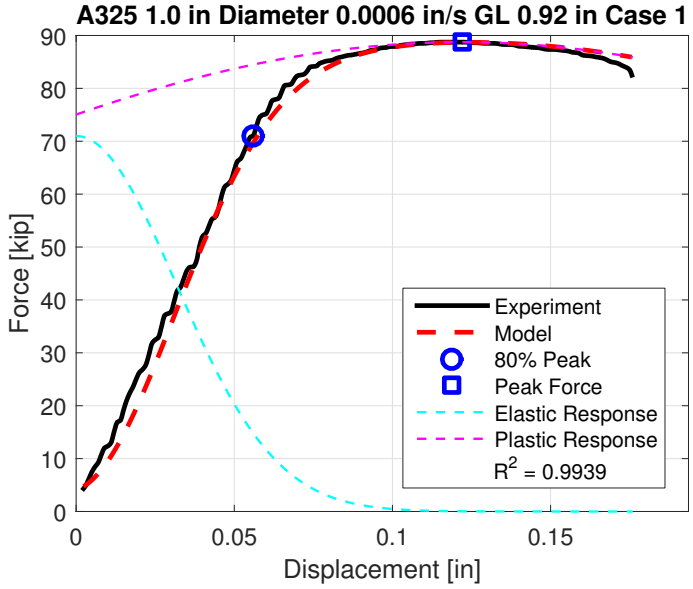

Figure A.44.

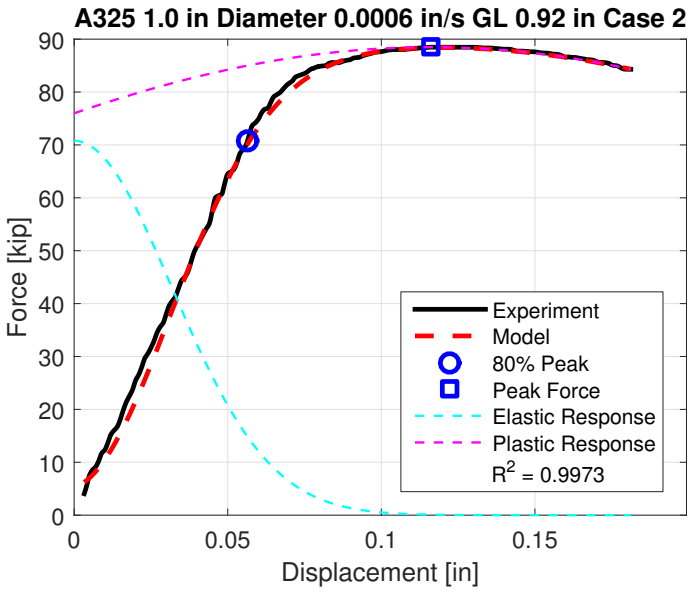

Figure A.45.

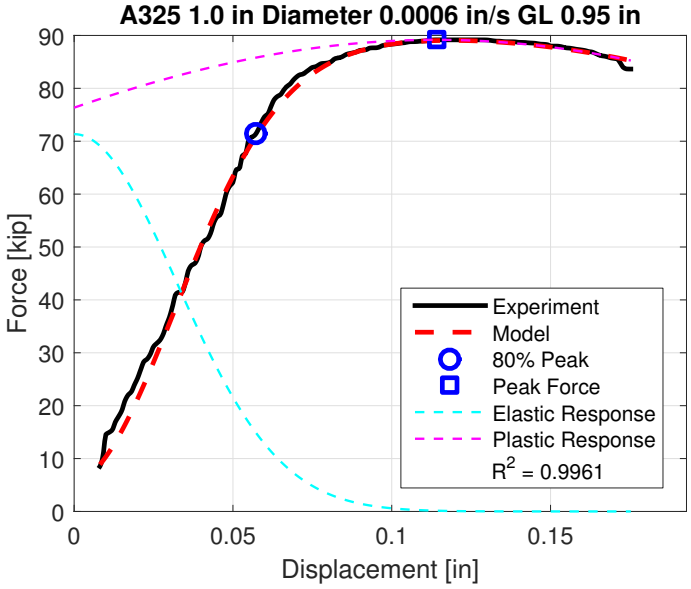

Figure A.46.

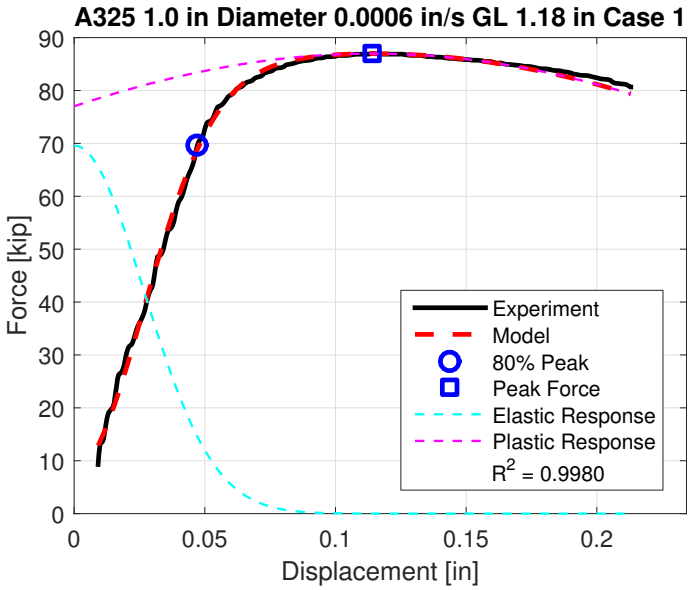

Figure A.47.

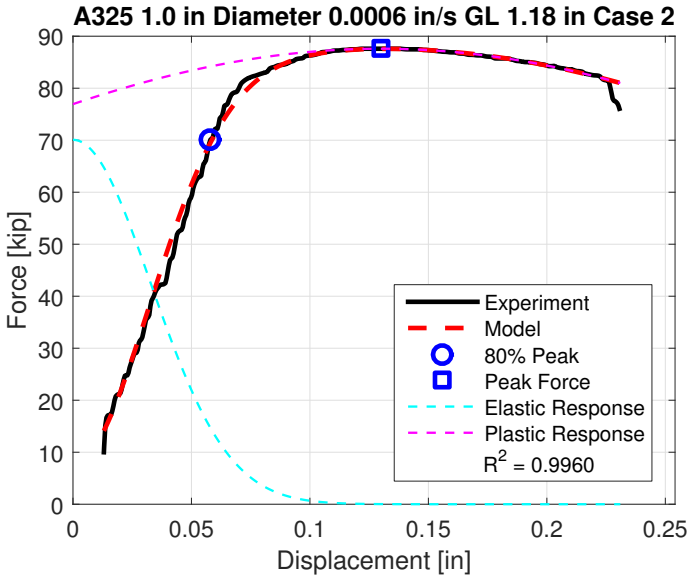

Figure A.48.

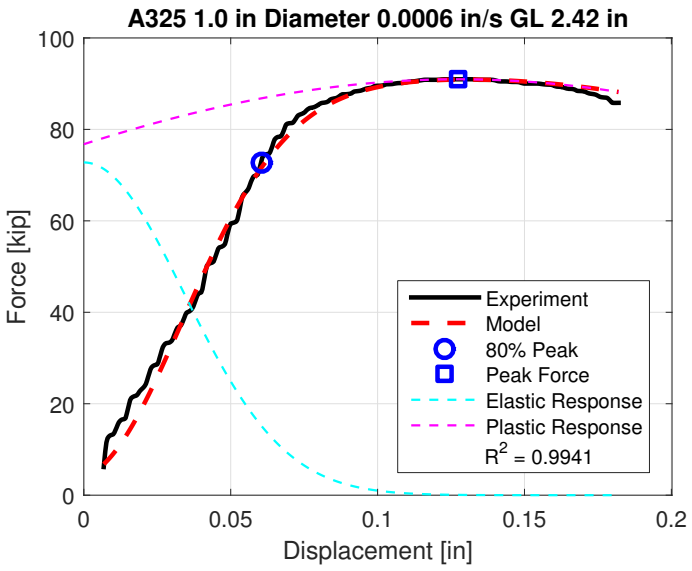
A325 1.0 in Diameter 0.0006 in/s GL 2.42 in
Force [kip]
Displacement [in]
0
20
40
60
80
100
0
0.05
0.1
0.15
0.2
Experiment
Model
80% Peak
Peak Force
Elastic Response
Plastic Response
R2 = 0.9941

Figure A.49.

A.4 A490 Results

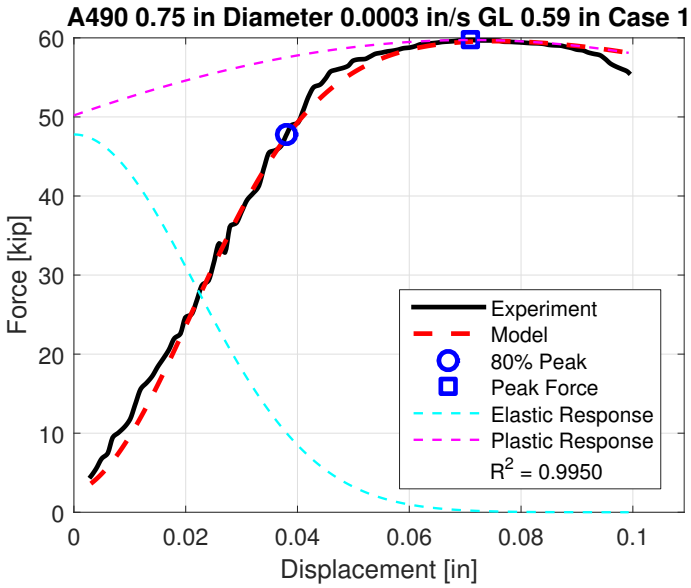

Figure A.50.

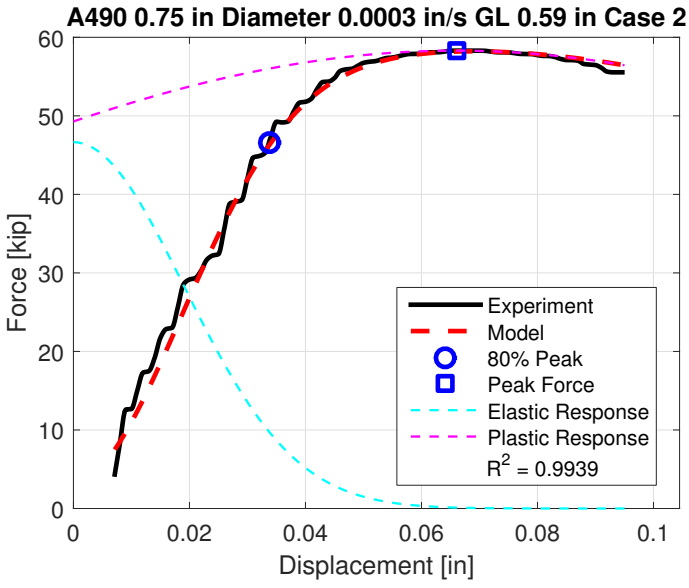

Figure A.51.

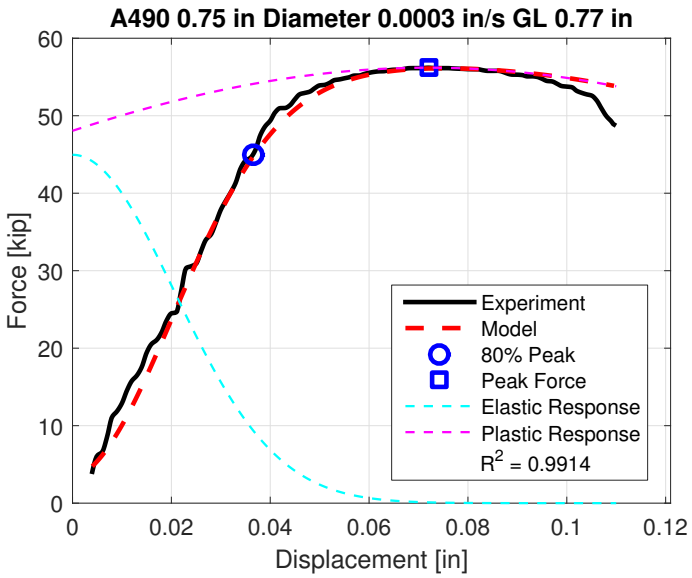

Figure A.52.

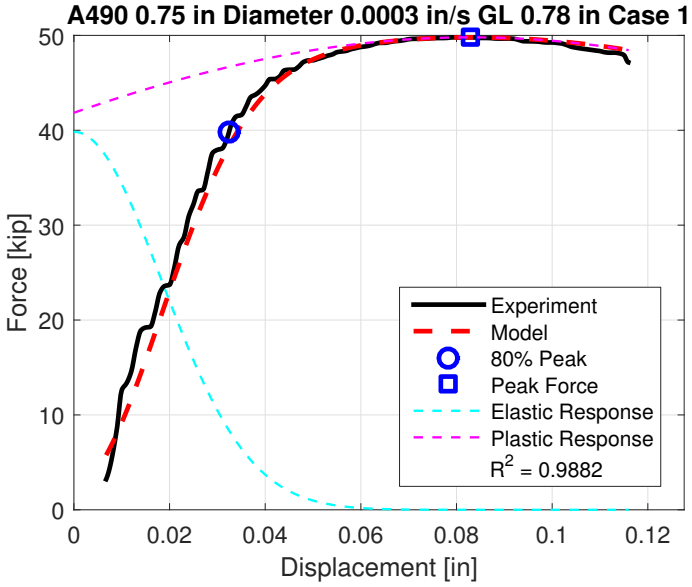

Figure A.53.

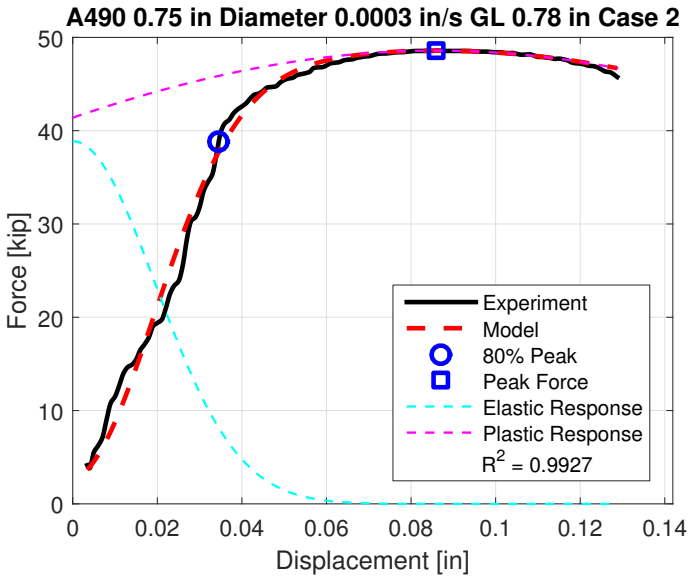

Figure A.54.

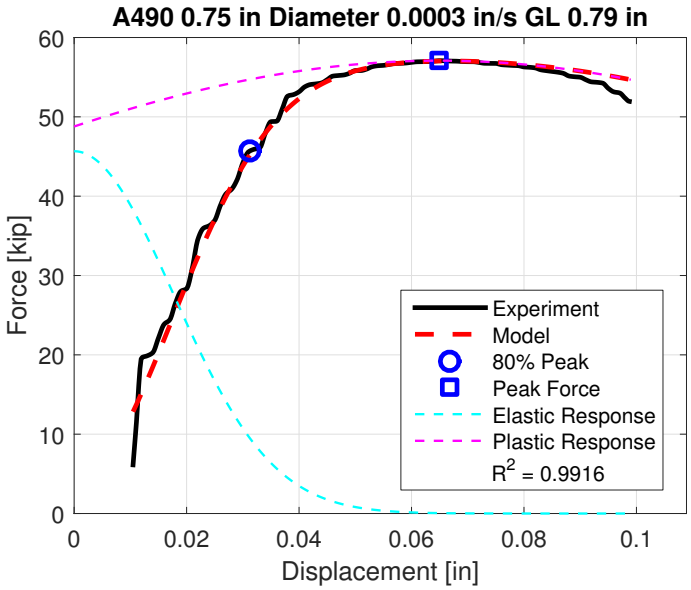

Figure A.55.

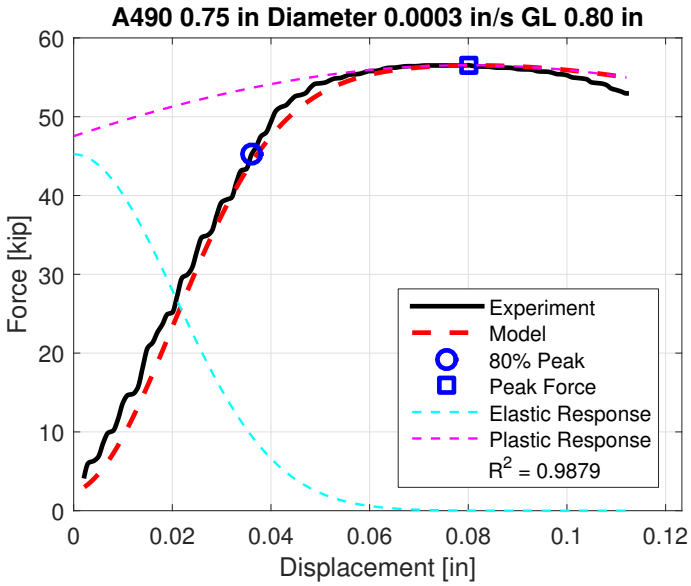

Figure A.56.

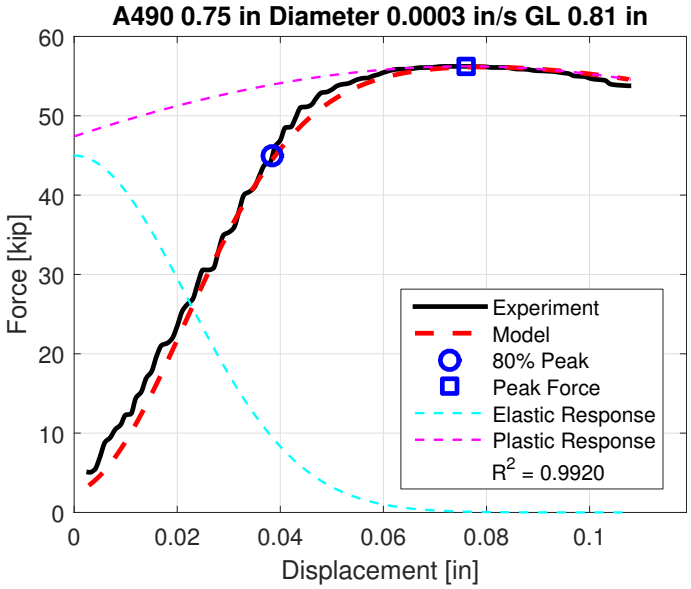

Figure A.57.

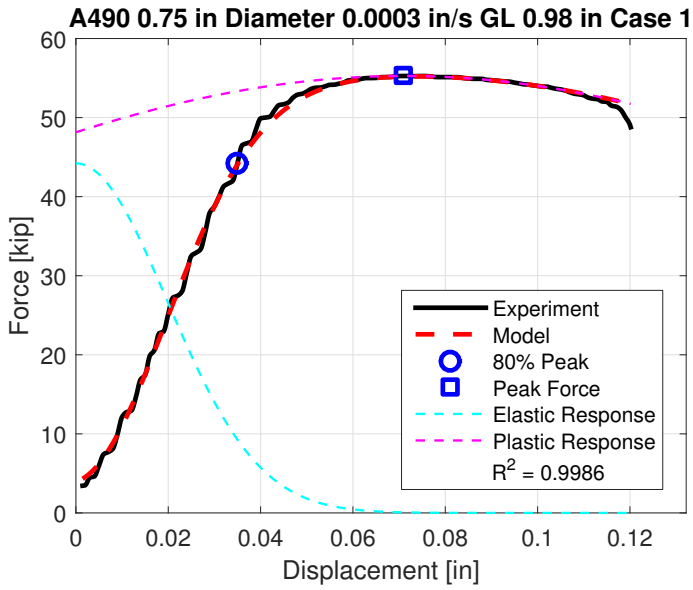

Figure A.58.

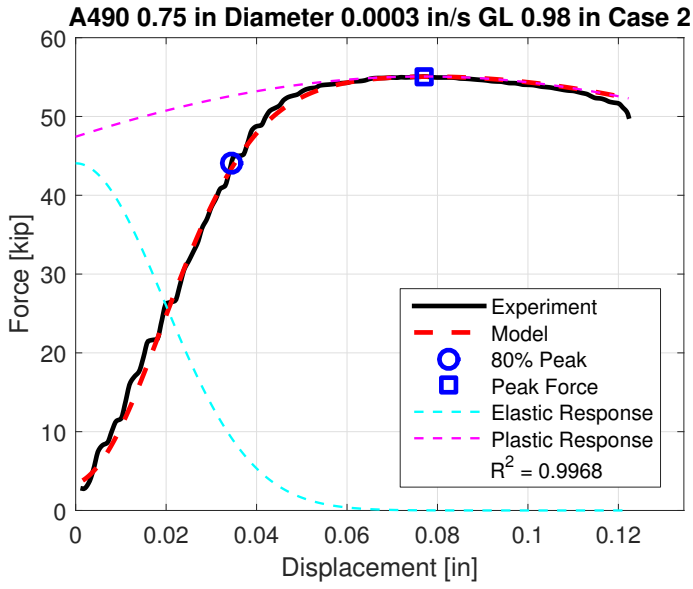

Figure A.59.

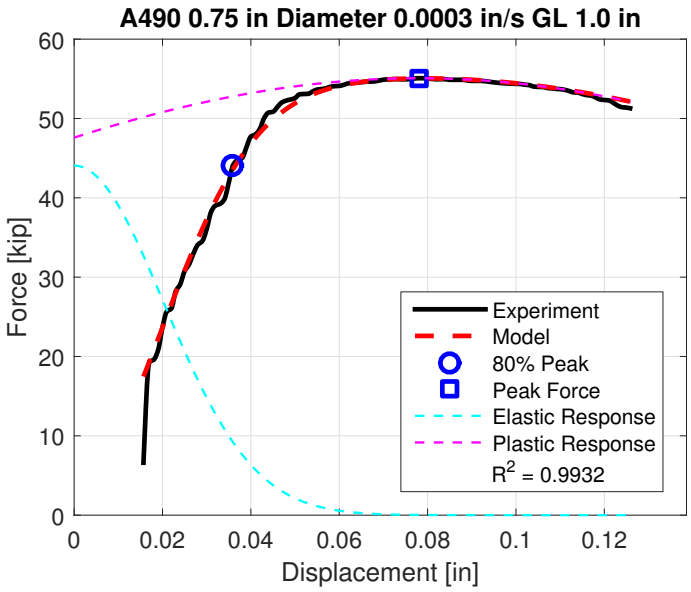

Figure A.60.

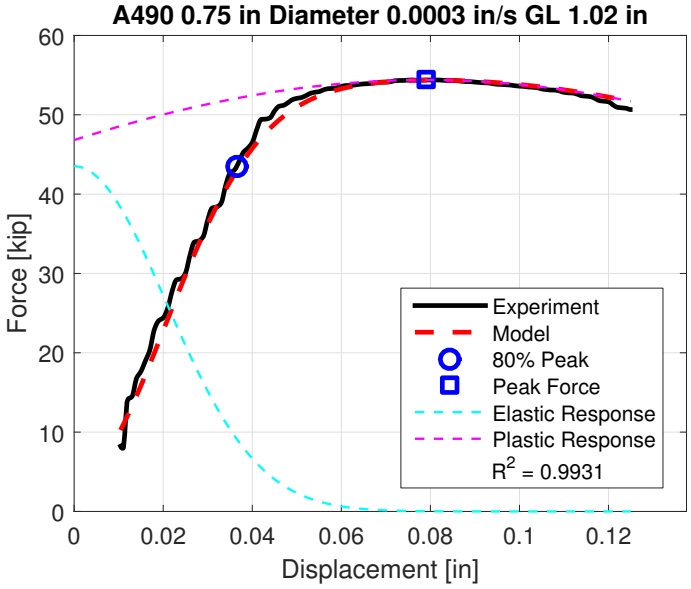

Figure A.61.

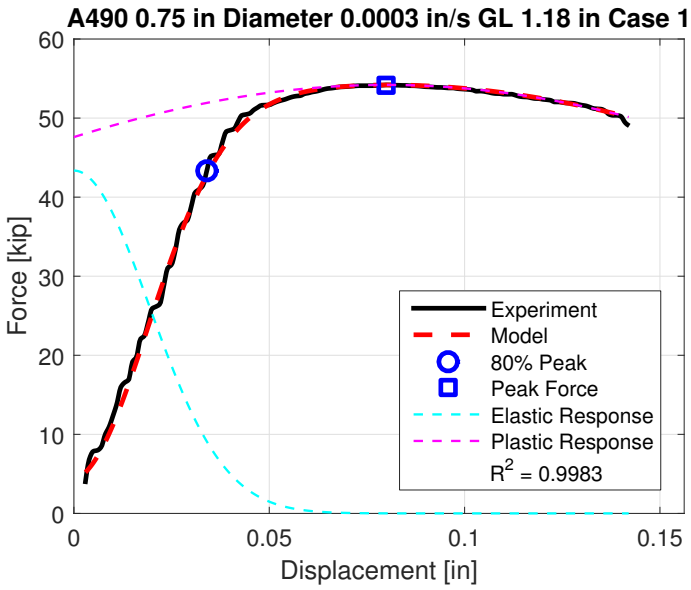

Figure A.62.

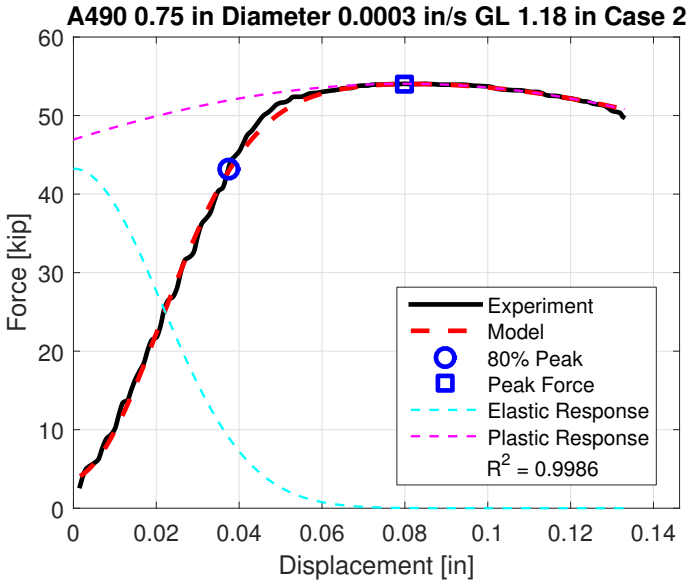

Figure A.63.

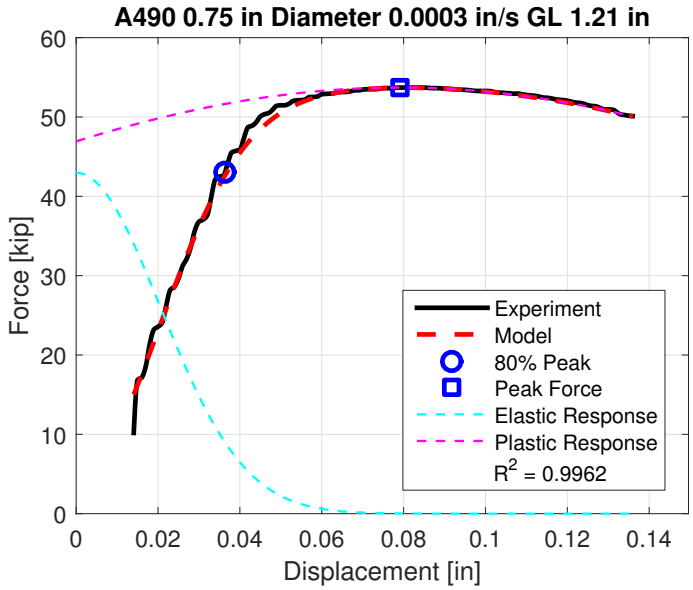

Figure A.64.

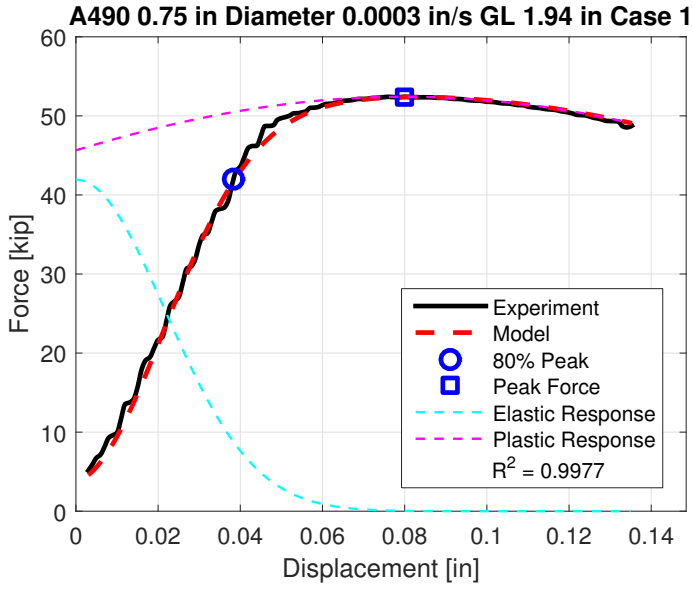

Figure A.65.

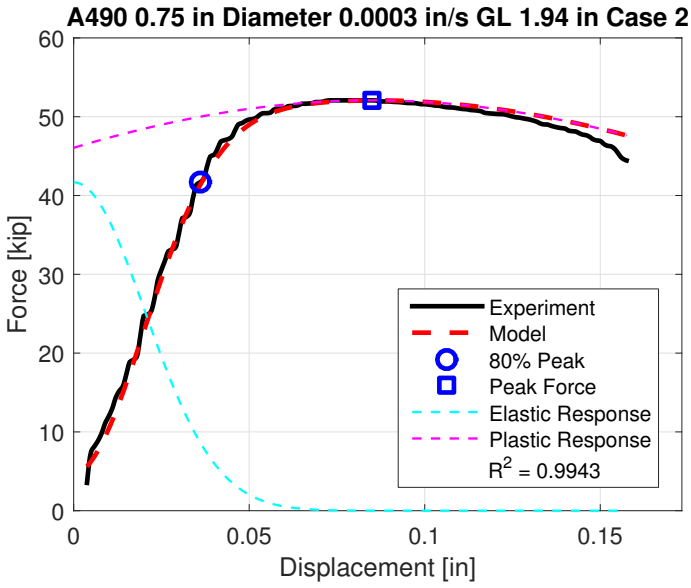

Figure A.66.

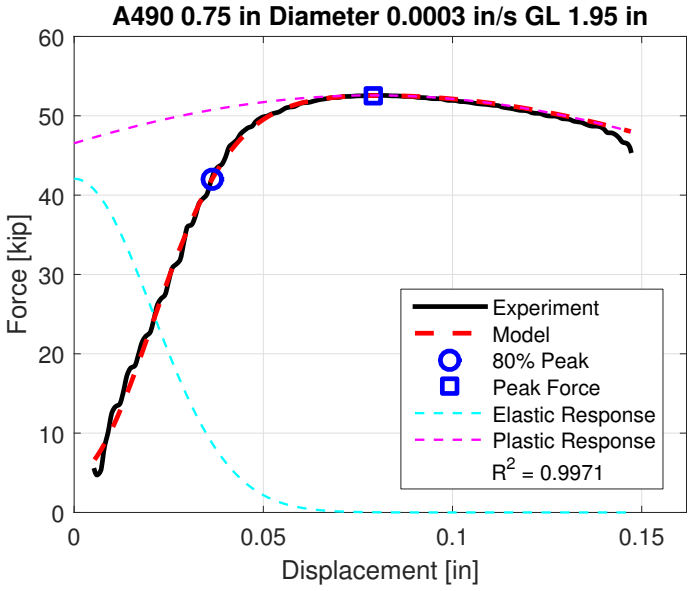

Figure A.67.

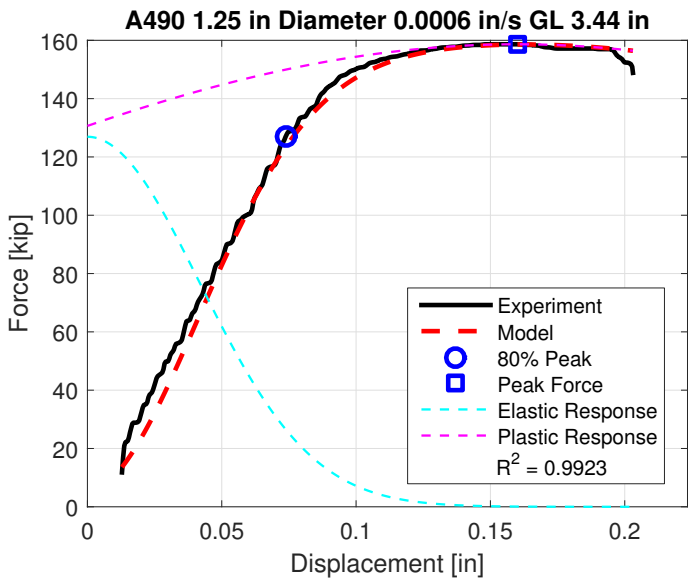

Figure A.68.

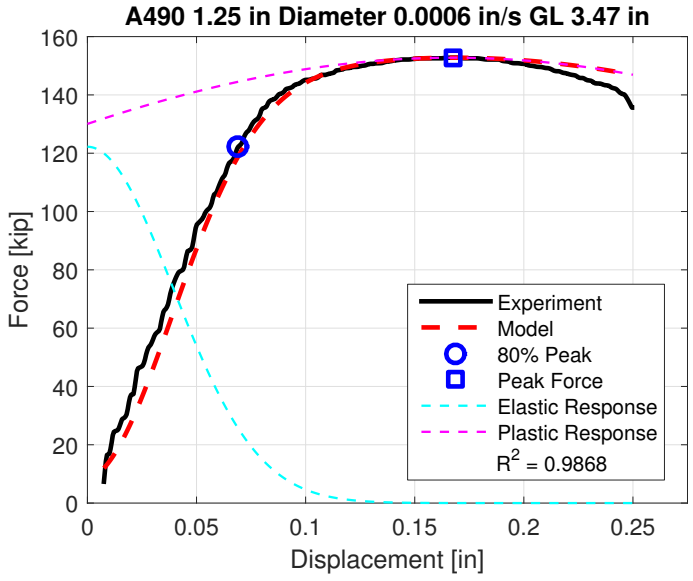

Figure A.69.

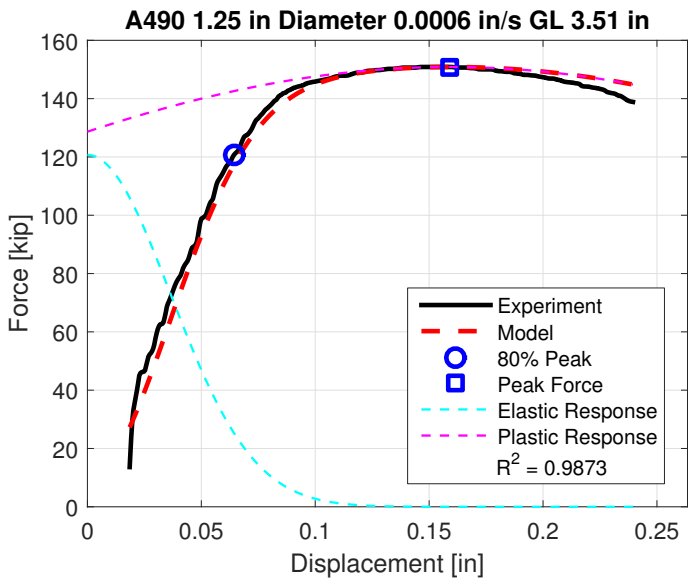

Figure A.70.

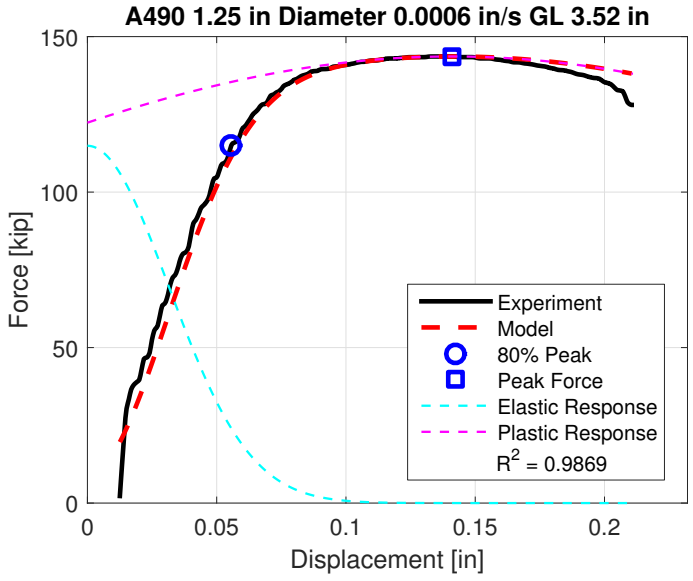

Figure A.71.

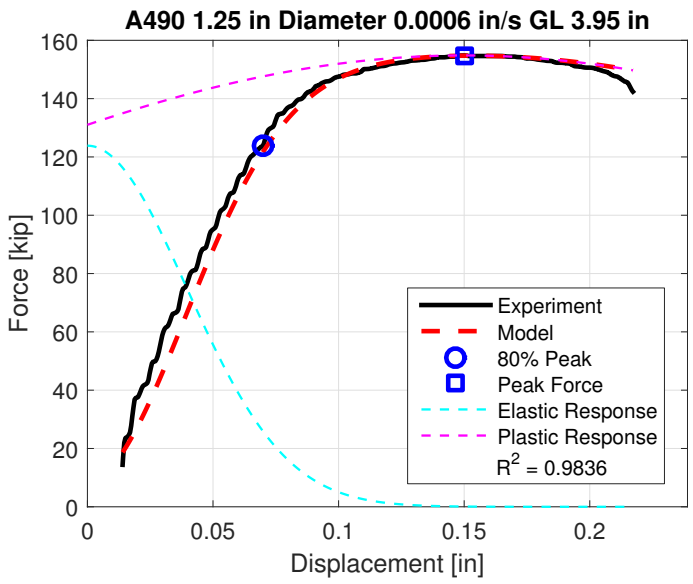

Figure A.72.

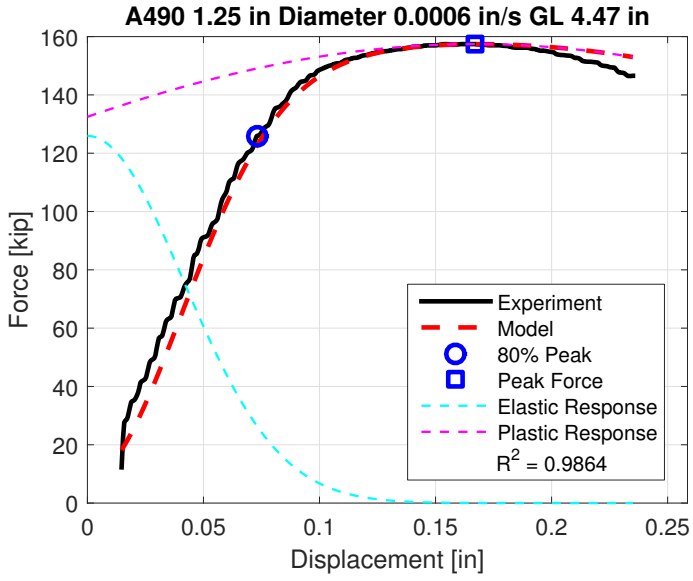

Figure A.73.

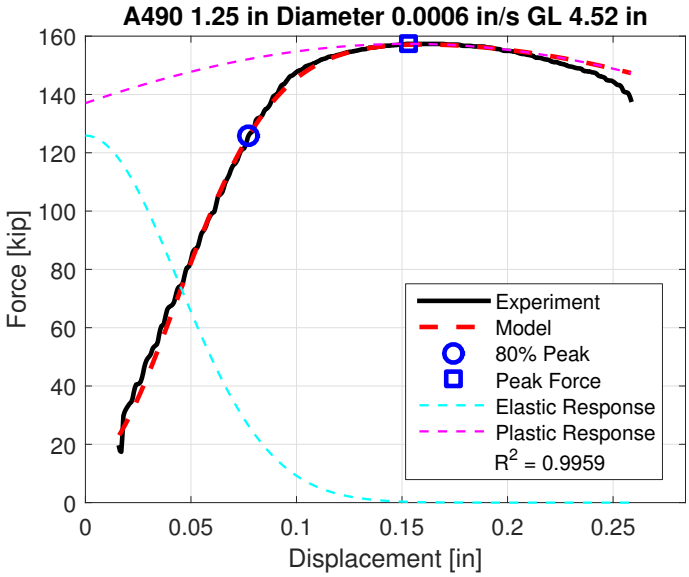
A490 1.25 in Diameter 0.0006 in/s GL 4.52 in
Force [kip]
Displacement [in]
Experiment
Model
80% Peak
Peak Force
Elastic Response
Plastic Response
R2 = 0.9959

Figure A.74.

B Appendix: High Ductility Model Results

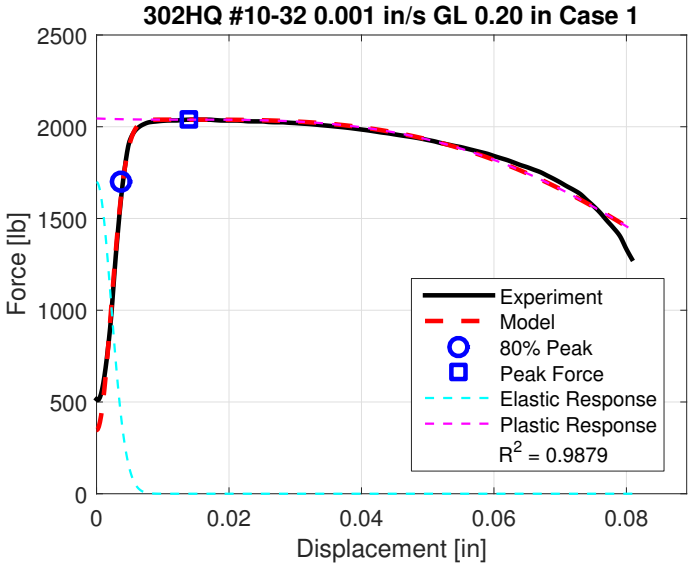

Figure B.1.

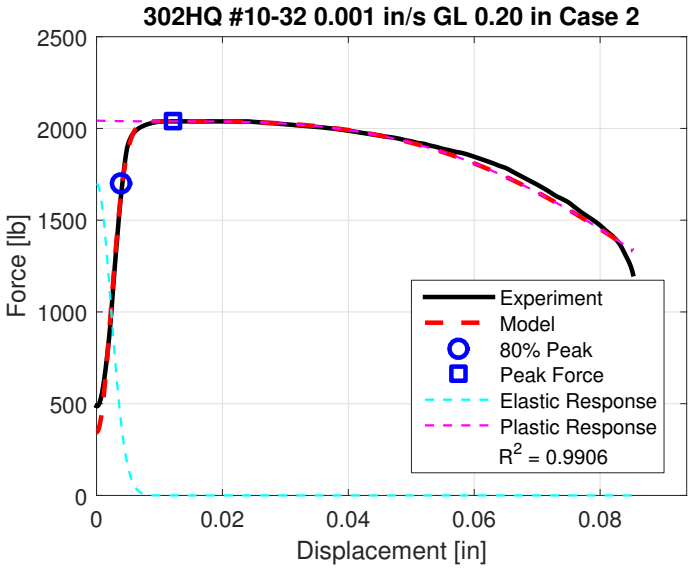

Figure B.2.

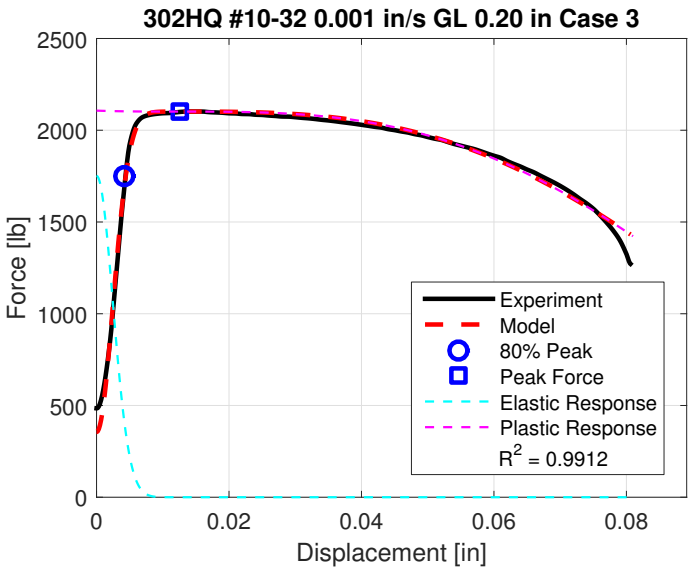

Figure B.3.

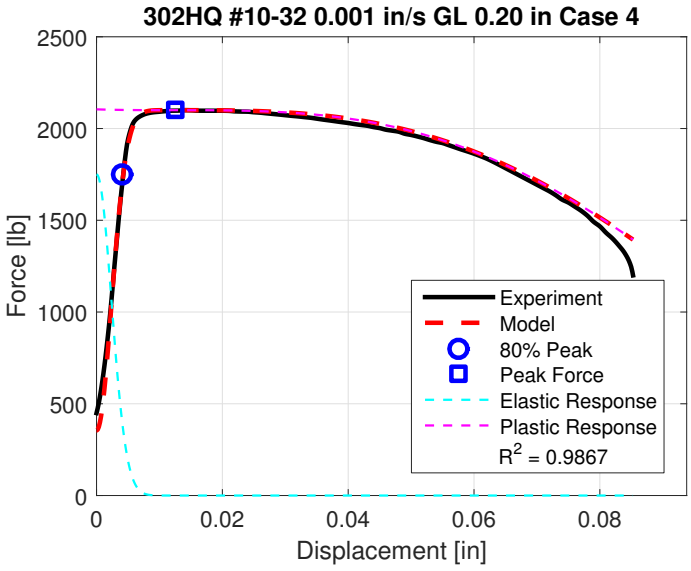

Figure B.4.

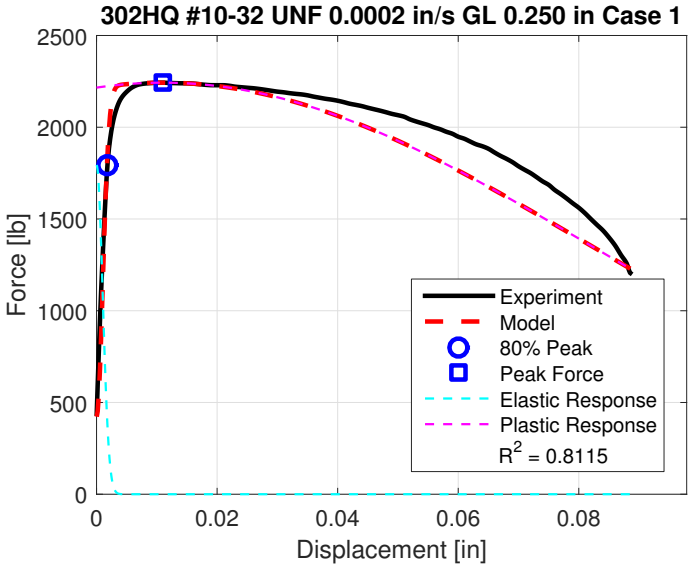

Figure B.5.

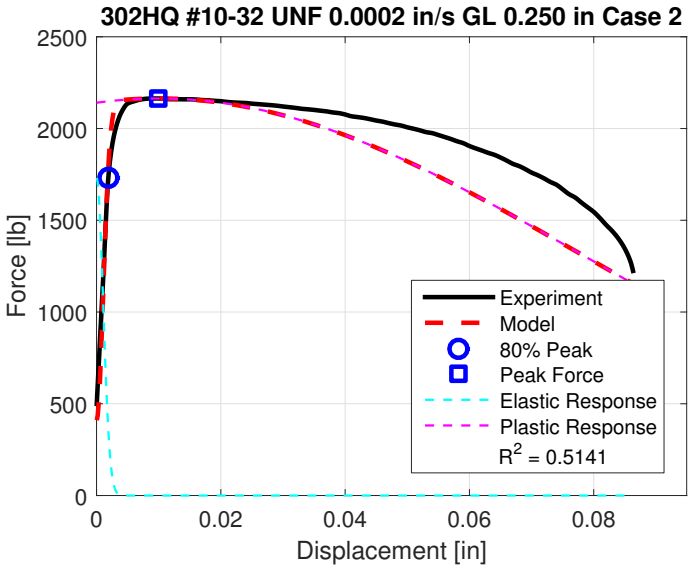

Figure B.6.

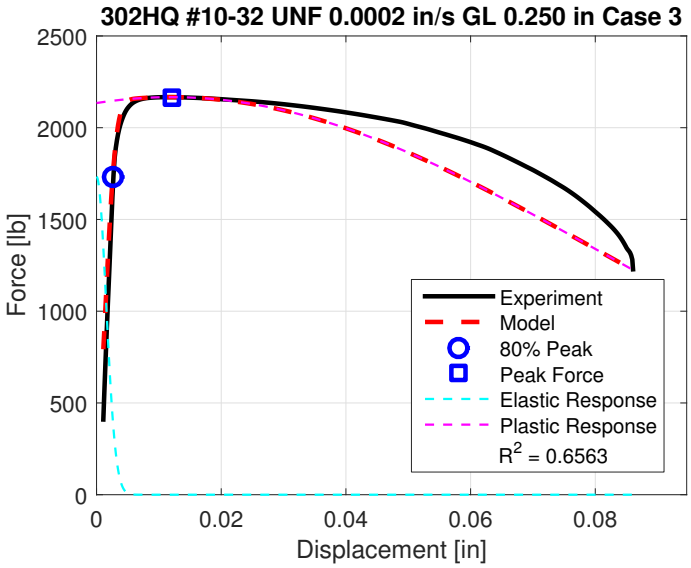

Figure B.7.

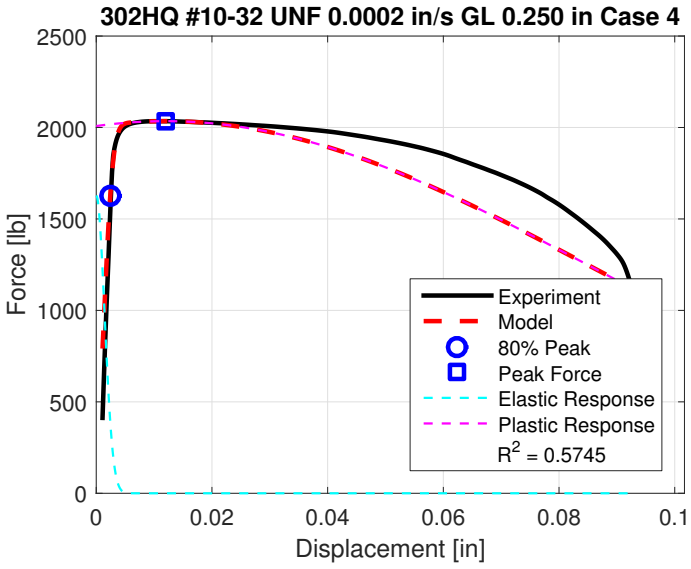

Figure B.8.

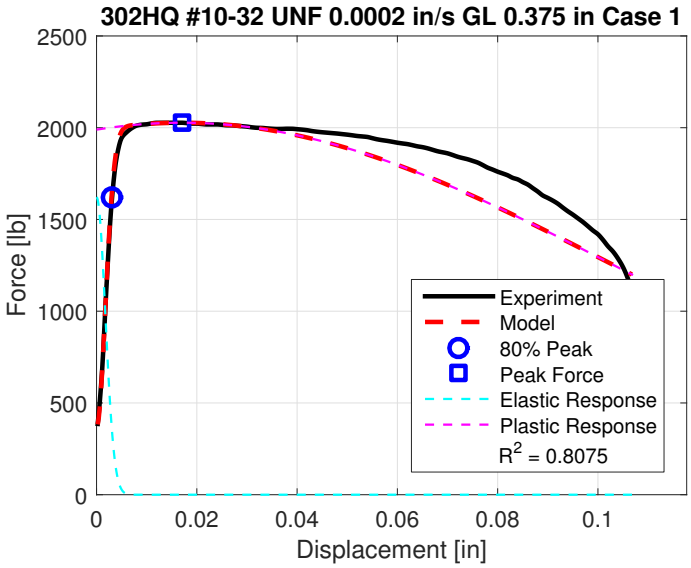

Figure B.9.

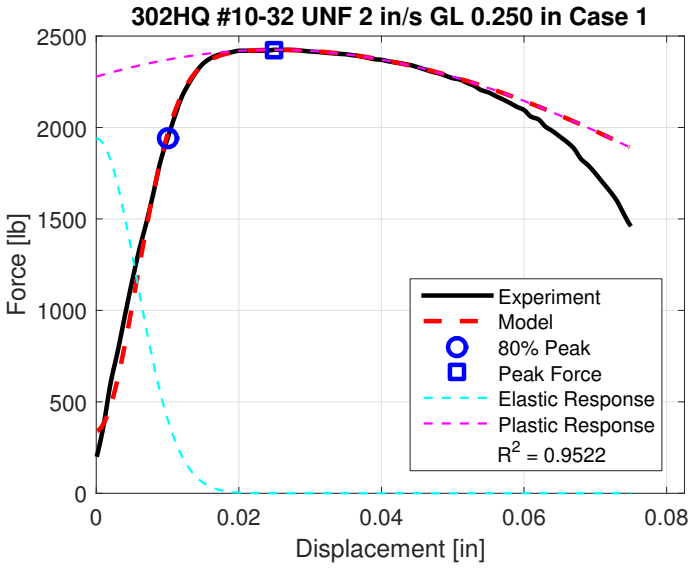

Figure B.10.

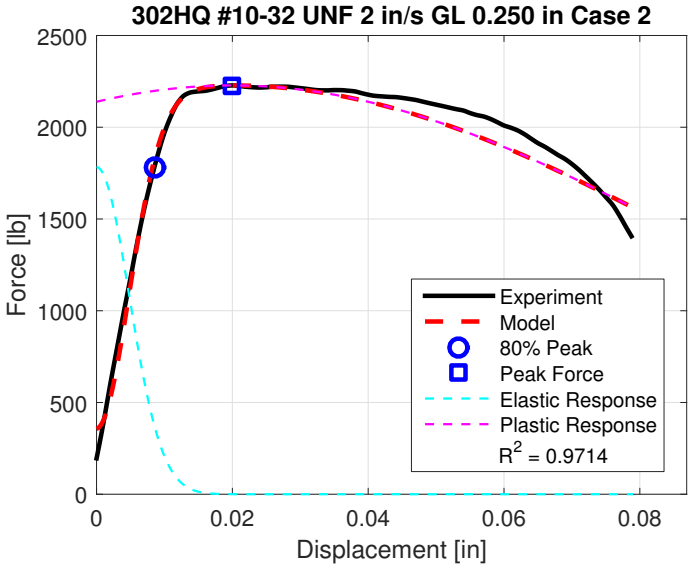

Figure B.11.

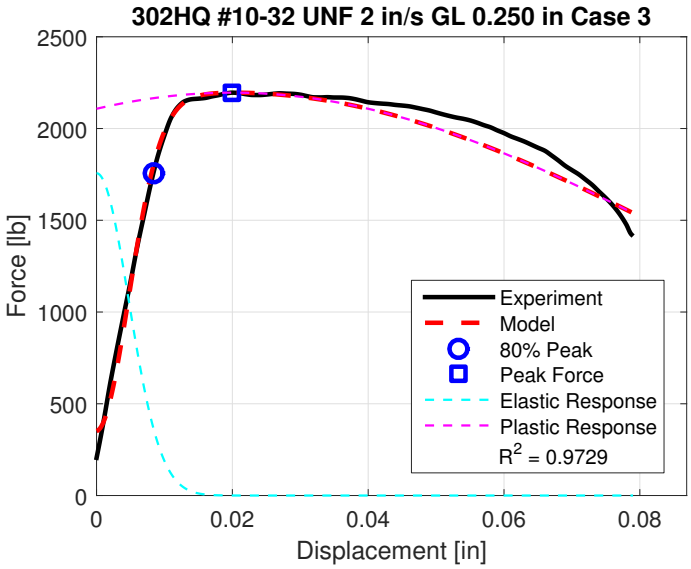

Figure B.12.

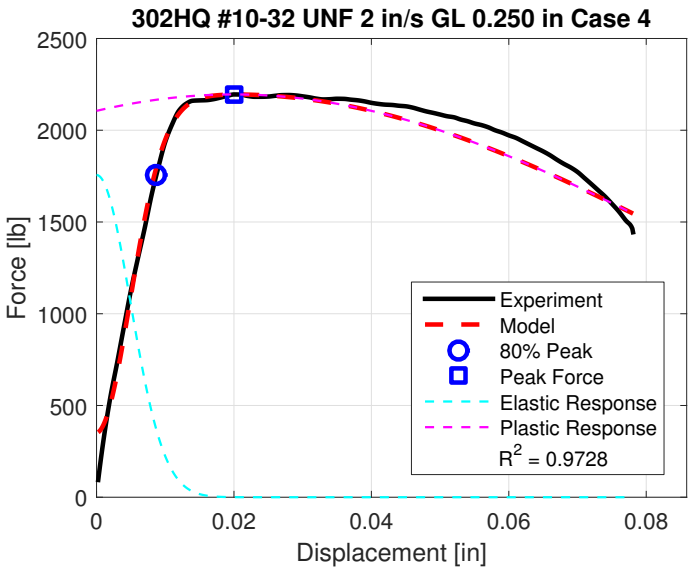

Figure B.13.

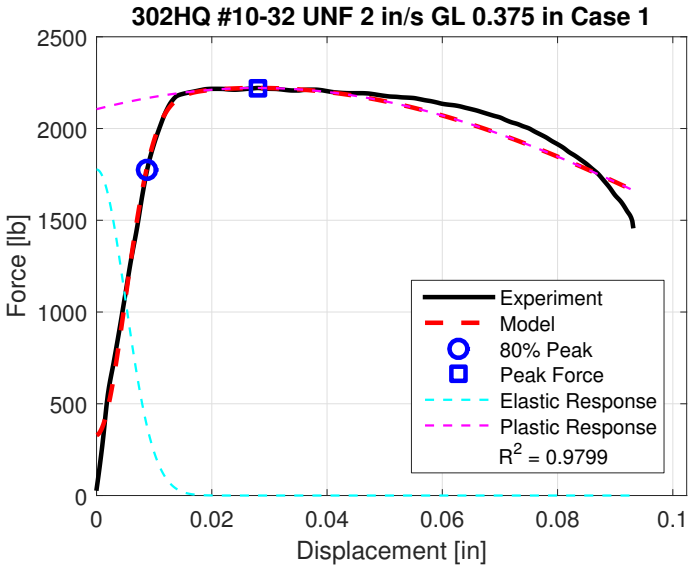

Figure B.14.

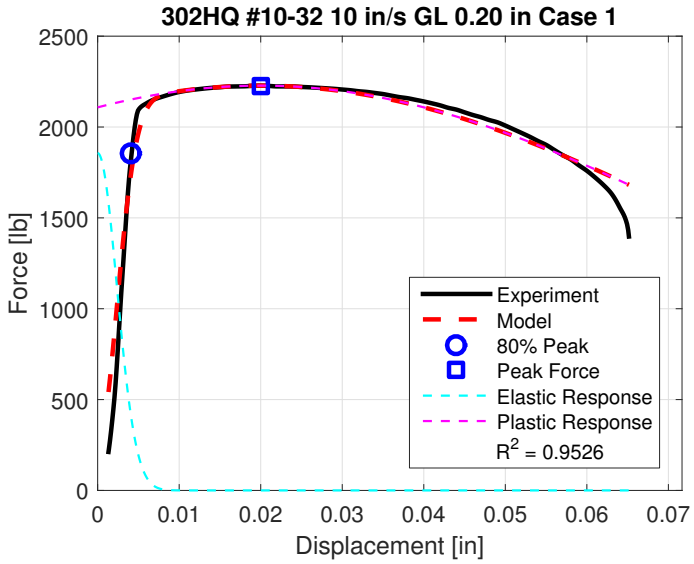

Figure B.15.

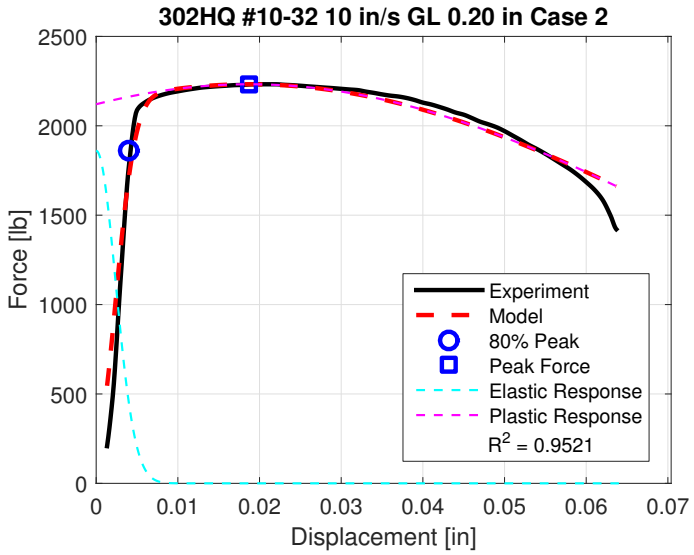

Figure B.16.

C Appendix: MATLAB Scripts

C.1 Force Displacement Curve

```
function Force = FastenerFailureROM(d,F,Ductile)
if nargin == 2
Ductile = 1;
end

if Ductile == 1
gamma = 2;
else
gamma = 3;
end

Fp = max(F); % Find peak force
dp = d(F == max(F)); % Find peak displacement

% If peak force occurs at multiple displacements, we will use the average
% of these displacements.
if length(dp) > 1
dp2 = mean(dp);
dp = [];
dp = dp2;
end

df = d(end); % Find fracture displacement

% Try to interpolate delta_80, but if this produces an error we will
% instead use the nearest displacement below delta_80.
try
d80 = interp1(F(d < dp),d,4/5*Fp);
catch
d80 = d(sum(F(d < dp) <= 4/5*Fp));
end

% Compute resulting force curve
Force = Fp*(-4/5*exp(-(5/4*d/d80).^2)+exp(-((d-dp)/(df+dp)).^gamma));
```

C.2 Output Force Given Displacement Point

```
function Force = FastenerFailureROM(d,F,disp,Ductile)
%% Outputs a single force at the given displacement disp.
% d is the entire displacement vector from the force displacement curve.
% F is the entire force vector from the force displacement curve.
% disp is a single displacment value used to compute the current force.
% Ductile determines whether a high strength or high ductility model is
% used.
% Ductile = 1 -> High strength (Default)
% Ductile = 2 -> High ductility
if nargin == 2
Ductile = 1;
end

if Ductile == 1
gamma = 2;
else
gamma = 3;
end

Fp = max(F); % Find peak force
dp = d(F == max(F)); % Find peak displacement

% If peak force occurs at multiple displacements, we will use the average
% of these displacements.
if length(dp) > 1
dp2 = mean(dp);
dp = [];
dp = dp2;
end

df = d(end); % Find fracture displacement

% Try to interpolate delta_80, but if this produces an error we will
% instead use the nearest displacement below delta_80.
try
d80 = interp1(F(d < dp),d,4/5*Fp);
catch
d80 = d(sum(F(d < dp) <= 4/5*Fp));
end

% Compute resulting force curve
Force = Fp*(-4/5*exp(-(5/4*disp/d80).^2)+exp(-((disp-dp)/(df+dp)).^gamma));
```

DISTRIBUTION:

1	MS 0346	Organization 1526, (electronic)
1	MS 0557	C. Dennis Croessmann, 1520 (electronic)
1	MS 1070	The Fastener Working Group, (electronic)
1	MS 0899	Technical Library, 9536 (electronic copy)

Sandia National Laboratories